Raman scattering of light by polaritons

Yu. N. Polivanov

P. N. Lebedev Physics Institute, Academy of Sciences of the USSR, Moscow
Usp. Fiz. Nauk **126**, 185–232 (October 1978)

The main results are given of the experimental and theoretical investigations demonstrating the capabilities and characteristics of the spectroscopy utilizing spontaneous Raman scattering of light by polaritons. The following topics are considered: polariton dispersion; frequency-angular scattering spectra; experimental methods; intensity and line shape of scattered light; relationship of the Raman scattering of light by polaritons to the Raman scattering by optical phonons, to second harmonic generation, and to the linear electrooptic effect; characteristics of polariton spectra due to free carriers, localized modes, energy bands of two-particle states, and gyrotropy of crystals; coherent anti-Stokes Raman scattering of light by polaritons.

PACS numbers: 78.30. – j, 71.36. + c, 42.65.Cq

CONTENTS

1. INTRODUCTION

The recent rapid growth of investigations of the properties of elementary excitations in crystals owes its origin to the introduction of lasers in optics. Raman scattering of light has become one of the main investigation methods. The last few years have seen intensive investigations of the Raman scattering of light not only by optical phonons (this has also been done earlier) but also by polaritons, which can be observed only when laser excitation sources are used.

Raman scattering has now become an effective method for investigating the characteristics of the spectra of polariton excitations and of their changes as a result of interactions of polaritons with other elementary excitations and with many-particle states in solids. Studies of Raman scattering by polaritons have given information on important parameters of solids, such as the dispersion of the permittivity and of the nonlinear susceptibility, which describes the scattering intensity over a wide spectral range including lattice resonances. Moreover, such investigations have helped in the development of tunable stimulated radiation sources emitting in the medium and far infrared as a result of stimulated Raman scattering by polaritons or as a result of generation of difference frequencies in the polariton part of the spectrum.

Raman scattering of light by polaritons was first observed experimentally in 1965 by Henry and Hopfield,[1] who studied a cubic crystal of GaP. Since that time, experimental studies of Raman scattering have been made in cubic, uniaxial, and biaxial crystals. The investigated cubic crystals include gallium phosphide GaP (Refs. 1 and 3), gallium arsenide GaAs (Ref. 4), sodium chlorate and bromate $NaClO_3$ and $NaBrO_3$ (Ref. 5), hexamethylenetetramine $(CH_2)_6N_4$ (Ref. 6), ammonium chloride NH_4Cl (Refs. 7 and 8), as well as centrosymmetric cubic crystals of strontium titanate $SrTiO_3$ (Ref. 10), and potassium tantalate $KTaO_3$ (Ref. 10), in which the Raman scattering of light is activated by an external

 0038-5670/78/100805-27$01.10 © 1980 American Institute of Physics

electric field. The uniaxial crystals include zince oxide ZnO (Refs. 2 and 23), quartz α-SiO_2 (Refs. 11 and 12) and β-SiO_2 (Ref. 12), lithium niobate $LiNbO_3$ (Refs. 13–22), barium titanate $BaTiO_3$ (Refs. 24–27, 103, 118, and 119), lithium iodate $LiIO_3$ (Refs. 28–40), zince selenide ZnSe (Refs. 41 and 42), lithium tantalate $LiTaO_3$ (Refs. 43–45 and 113), potassium cyanocuprate $K_3Cu(CN)_4$ (Refs. 46, 47, and 49), cadmium sulfide CdS (Refs. 50 and 51), beryllium oxide BeO (Ref. 52), barium nitrite $Ba(NO_2)_2 \cdot H_2O$ (Ref. 53), and paratellurite TeO_2 (Ref. 163). The following biaxial crystals have also been studied: iodic acid α-HIO_3 (Refs. 54–57), barium-sodium niobate $Ba_2NaNb_5O_{15}$ (Ref. 58), potassium-barium-sodium niobate $K_{1-x}Na_xBa_2Nb_5O_{15}$ (Ref. 59), metadinitrobenzene $C_6H_4(NO_2)_2$ (Ref. 61), metanitroaniline NO_2-C_6H_4-NH_2 (Ref. 62), potassium niobate $KNbO_3$ (Refs. 63–67), lead titanate $PbTiO_3$ (Ref. 68), lithium formate $LiCOOH \cdot H_2O$ (Refs. 60, 80, and 81), and barium formate $Ba(COOH)_2$ (Ref. 78).

In this connection it is also worth mentioning the parametric scattering of light, which is effectively the Raman scattering of light by polaritons of the "photon-like" part of the upper polariton branch. Parametric scattering was first discovered in 1967 independently at three universities: Moscow,[114,115] Stanford,[116] and Cornell.[117] In these first experiments the scattering of light was observed in crystals of potassium dihydrogen phosphate KH_2PO_4 (Ref. 114), lithium niobate $LiNbO_3$ (Refs. 115 and 116), and ammonium dihydrogen phosphate $NH_4H_2PO_4$ (Ref. 117). A review of some of the work on parametric scattering of light can be found in Refs. 83 and 139.

We shall systematically review, on the basis of the published experimental and theoretical results, the main ideas necessary for the understanding of the characteristics and potentialities of the spectroscopy of the spontaneous Raman scattering of light by polaritons. We shall also describe the methods for experimental investigation of this scattering. The stimulated scattering of light by polaritons deserves a separate review and it will not be discussed here.

2. POLARITON DISPERSION

Some optical vibration modes of the crystal lattice induce electric polarization. They are called the polar vibrations. These vibrations are accompanied by the appearance of electromagnetic waves which interact strongly with mechanical vibrations. The equations of motion for the polar vibrations should therefore describe both the displacements of ions relative to one another and the components of the associated electromagnetic field.

a) Cubic diatomic crystals

These equations of motion were first solved simultaneously by Born and Huang[69] for the diatomic lattice of a cubic ionic crystal. The equations of motion for this lattice are as follows:

$$\left.\begin{array}{ll} \ddot{\mathbf{w}}=b_{11}\mathbf{w}+b_{12}\mathbf{E}, & \mathbf{P}=b_{21}\mathbf{w}+b_{22}\mathbf{E}, \\ \operatorname{div}\mathbf{D}=0, & \operatorname{div}\mathbf{H}=0, \\ \operatorname{curl}\mathbf{E}=-\frac{1}{c}\dot{\mathbf{H}}, & \operatorname{curl}\mathbf{H}=\frac{1}{c}\dot{\mathbf{D}}, \end{array}\right\} \tag{2.1}$$

where $\mathbf{w}=\mathbf{u}\sqrt{m_1m_2/(m_1+m_2)}$; $\mathbf{u}$ is the vector representing the displacements of the two sublattices relative to one another; m_1 and m_2 are the masses of the atoms; b_{11}, b_{12}, b_{21}, and b_{22} are certain coefficients; the rest of the notation is standard.

The equation for the relative displacements of ions and the Maxwell equations describe the simultaneous (mixed) optical vibrations of an ionic crystal and oscillations of the associated electromagnetic field. Therefore, this system of equations makes it possible to take into account, in the simplest form, the interaction between photons and optical phonons.

It is known from electrodynamics that the displacement field $\mathbf{w}$ can be eliminated from the Maxwell equations by introducing the permittivity of the medium ε relating the time-dependent Fourier components of the vectors $\mathbf{D}$ and $\mathbf{E}$:

$$\mathbf{D}(\omega)=\varepsilon(\omega)\,\mathbf{E}(\omega). \tag{2.2}$$

We shall seek the solution of the system (2.1) in the approximation of plane monochromatic waves, i.e., we shall assume that w, P, E, and H all vary proportionally to $\exp[i\mathbf{k}\cdot\mathbf{r}-\omega t]$. In this case, we find from Eq. (2.1) that

$$\left.\begin{array}{ll} -\omega^2\mathbf{w}=b_{11}\mathbf{w}+b_{12}\mathbf{E}, & \mathbf{P}=b_{21}\mathbf{w}+b_{22}\mathbf{E}, \\ (\mathbf{k}\cdot\mathbf{D})=\mathbf{k}(\mathbf{E}+4\pi\mathbf{P})=0, & (\mathbf{k}\cdot\mathbf{H})=0, \\ [\mathbf{k}\times\mathbf{E}]=\frac{\omega}{c}\mathbf{H}, & [\mathbf{k}\times\mathbf{H}]=-\frac{\omega}{c}(\mathbf{E}+4\pi\mathbf{P})=-\frac{\omega}{c}\mathbf{D}. \end{array}\right\} \tag{2.3}$$

Hence, using Eq. (2.2), we can write down the following expressions for $\mathbf{w}$, $\mathbf{P}$, and $\mathbf{D}$:

$$\mathbf{w}=-\frac{b_{12}}{b_{11}+\omega^2}\mathbf{E}, \tag{2.4}$$

$$\mathbf{P}=\left(b_{22}-\frac{b_{12}b_{21}}{b_{11}+\omega^2}\right)\mathbf{E}, \tag{2.5}$$

$$\mathbf{D}=\left(1+4\pi b_{22}-\frac{4\pi b_{12}b_{21}}{b_{11}+\omega^2}\right)\mathbf{E}=\varepsilon\mathbf{E}. \tag{2.6}$$

It follows from Eq. (2.6) that

$$\varepsilon(\omega)=1+4\pi b_{22}-\frac{4\pi b_{12}b_{21}}{b_{11}+\omega^2}. \tag{2.7}$$

We shall compare this expression with the dispersion formula for the permittivity:

$$\varepsilon(\omega)=\varepsilon_\infty+\frac{S\omega_0^2}{\omega_0^2-\omega^2}=\varepsilon_\infty+\frac{\varepsilon_0-\varepsilon_\infty}{\omega_0-\omega^2}\omega_0^2, \tag{2.8}$$

where ε_0 is the static permittivity; ε_∞ is the permittivity at frequencies much higher than ω_0 but lower than the electron transition frequencies (subject to certain restrictions, we can regard ε_∞ as the square of the optical refractive index); ω_0 is the natural frequency of a dipole-active vibration of the crystal lattice; S is the oscillator strength of the vibration. A comparison of Eqs. (2.7) and (2.8) gives

$$\left.\begin{array}{l} b_{11}=-\omega_0^2, \\ b_{12}=b_{21}=\sqrt{\frac{\varepsilon_0-\varepsilon_\infty}{4\pi}}\omega_0, \\ b_{22}=\frac{1}{4\pi}(\varepsilon_\infty-1). \end{array}\right\} \tag{2.9}$$

The solution of the system (2.3) represents a combination of longitudinal and transverse waves. In fact, using Eq. (2.5), we can transform the third equation of the system (2.3) to

$$(\mathbf{k}\cdot\mathbf{E})\left(1+4\pi b_{22}-\frac{4\pi b_{12}b_{21}}{b_{11}+\omega^2}\right)=0. \tag{2.10}$$

Hence, we have two possibilities:

$$\text{A.}\quad 1+4\pi b_{22}-\frac{4\pi b_{12}b_{21}}{b_{11}+\omega^2}=0, \tag{2.11}$$

$$\text{B.}\quad (\mathbf{k}\cdot\mathbf{E})=0. \tag{2.12}$$

We shall first consider case A. The condition (2.11) implies, in accordance with Eq. (2.6), that $\mathbf{D}=0$. In this case it follows from the last equation of the system (2.3) that $[\mathbf{k}\times\mathbf{H}]=0$, which means that $\mathbf{H}=0$ and this in turn gives $[\mathbf{k}\times\mathbf{E}]=0$. Since $\mathbf{E}\neq 0$ [the condition $\mathbf{E}=0$ gives only a trivial solution of the system (2.3)], we may conclude that $\mathbf{E}\parallel\mathbf{k}$. In this case it also follows from Eqs. (2.4) and (2.5) that $\mathbf{P}\parallel\mathbf{k}$ and $\mathbf{w}\parallel\mathbf{k}$. Thus, case A corresponds to longitudinal optical (*LO*) vibrations whose frequencies are governed by the solution of Eq. (2.11) and hence, using Eq. (2.9), we obtain

$$\omega^2=-b_{11}+\frac{4\pi b_{12}b_{21}}{1+4\pi b_{22}}=\frac{\varepsilon_0}{\varepsilon_\infty}\omega_0^2=\omega_L^2, \tag{2.13}$$

where ω_L is the frequency of a longitudinal optical phonon.

Case B corresponds to transverse optical (*TO*) vibrations ($\mathbf{E}\perp\mathbf{k}, \mathbf{P}\perp\mathbf{k}$). The dispersion relationship for the transverse vibrations can be obtained by multiplying vectorially the penultimate equation in the system (2.3) by k and applying the identity

$$[\mathbf{k}\times[\mathbf{k}\times\mathbf{E}]]=\mathbf{k}(\mathbf{k}\cdot\mathbf{E})-k^2E.$$

Finally, eliminating from the resultant equation the value of H and using Eqs. (2.2), (2.8), and (2.12) we find that

$$\frac{k^2c^2}{\omega}=\varepsilon(\omega)=\varepsilon_\infty+\frac{S\omega_0^2}{\omega_0^2-\omega^2}=\varepsilon_\infty+\frac{\varepsilon_0-\varepsilon_\infty}{\omega_0^2-\omega^2}\omega_0^2, \tag{2.14a}$$

which, together with Eq. (2.13), can also be written in the form

$$\frac{k^2c^2}{\omega^2}=\varepsilon_\infty\frac{\omega_L^2-\omega^2}{\omega_0^2-\omega^2}. \tag{2.14b}$$

The above relationship gives the frequency of the transverse optical vibrations which depends on the wave vector k.

The dispersion relationship or law (i.e., the dependence of the frequency ω on the wave vector k), described by Eqs. (2.13) and (2.14) is represented in Fig. 1 for the range of low values of the wave vectors corresponding to the center of the Brillouin zone ($k\ll\pi/a$, where a is the lattice period). The continuous horizontal line 1 represents the solution of (2.13) for the longitudinal vibrations (ω_L) and the longitudinal optical phonon branch. The continuous curves 4 and 5 correspond to the solution of Eq. (2.14) for the transverse vibrations. The dashed lines 2 and 3 give the dispersion of an electromagnetic wave (photons) and of the transverse optical phonons ($\omega_0\cong\omega_T$), respectively, in the case when the interaction between them is not taken into account.

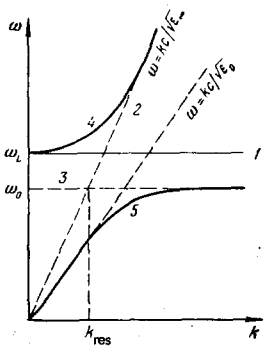

FIG. 1. Dispersion of longitudinal (1) and transverse (4, 5) optical vibrations in a diatomic cubic crystal near the center of the Brillouin zone ($k\ll\pi/a$) calculated allowing for the interaction between photons and polar optical phonons.

An interesting feature of the dispersion relationships of photons and phonons is that their graphs (the dashed lines 2 and 3 in Fig. 1) intersect. At the point of intersection ($\omega=\omega_0$ and $k=k_{res}$) the frequencies and wave vectors (wavelengths) of the different vibrations (oscillations) are identical. Therefore, even a weak interaction between them should give rise to a resonance which can have a considerable influence on the electromagnetic and mechanical processes in the investigated system.

In fact, the interaction between photons and phonons in a crystal gives rise to the appearance of two branches represented by the continuous curves 4 and 5 in Fig. 1. It is clear from this figure that at frequencies $\omega\gg\omega_L$ the upper dispersion branch reduces to the dispersion branch of photons in a crystal described by $\omega=kc/\sqrt{\varepsilon_\infty}$. Electromagnetic waves which have these frequencies in a crystal cannot set the lattice in motion because of its inertia. In this case the oscillation (vibration) energy is of electromagnetic nature. In the limit $k\to 0$ the frequency of the transverse lattice vibrations, described by the upper dispersion curve (4 in Fig. 1) tends to the frequency of the longitudinal optical phonons ($\omega\to\omega_L$) and the quantum energy is fundamentally mechanical.

At frequencies $\omega\ll\omega_0$, the lower branch (curve 5 in Fig. 1) is described by the dispersion relationship of electromagnetic waves in a medium with a certain static permittivity (Fig. 1). At such very low frequencies the lattice can follow completely the electromagnetic oscillations and this simply reduces the electromagnetic wave velocity. However, since the frequency is far from resonance, the mechanical displacements of the ions are small and the energy of the resultant excitations is basically electromagnetic. Conversely, if $\omega\to\omega_0, k\gg k_{res}$, the ion displacements are large and the quantum energy of the excitation is mechanical.[1)] However, in the intermediate range of wave vectors k ($k\sim k_{res}$) the transverse lattice vibrations are mixed with electromagnetic oscillations. The energy of such a mixed state is of electromagnetic–mechanical nature and the corresponding quanta are known as *polaritons*.

Thus, photons and phonons in a medium can be regarded as the limiting cases of polaritons and, in general, *polaritons describe the dispersion of real photons in a medium if it exhibits polar (dipole-active) vibrations*.

[1)] The frequency range between ω_0 and ω_L corresponds to $\varepsilon<0$; electromagnetic radiation whose frequency falls within this interval is not transmitted by a crystal. A strong optical reflection band is observed in this range. Surface waves which can exist at these frequencies are discussed in detail in the relevant reviews[87,88] and will not be considered here.

b) Cubic polyatomic crystals

The number of optical phonons in a crystal containing s atoms in a unit cell is $3s-3$ (Ref. 70). The first generalization of the Huang model to the case of polyatomic cubic crystals was made by Barker[71] in 1964. Let us assume that out of $3s-3$ optical phonons there are n phonons which are nondegenerate polar vibrations. According to Barker,[71] generalization of Eqs. (2.8), (2.13), and (2.14) then gives

$$\varepsilon(\omega)=\varepsilon_\infty+\sum_{f=1}^{n}\frac{S_f\omega_{Tf}^2}{\omega_{Tf}^2-\omega^2} \tag{2.15}$$

and

$$\prod_{f=1}^{n}\frac{\omega_{Lf}^2}{\omega_{Tf}^2}=\frac{\varepsilon_0}{\varepsilon_\infty}, \tag{2.16}$$

$$\frac{k^2c^2}{\omega^2}=\varepsilon_\infty+\sum_{f=1}^{n}\frac{S_f\omega_{Tf}^2}{\omega_{Tf}^2-\omega^2}. \tag{2.17}$$

Equation (2.16) is known as the generalized Lyddane–Sachs–Teller (LST) relationship.

By way of illustration, Fig. 2 shows the polariton dispersion for a cubic crystal with three polar vibrations (ω_{T1}, ω_{T2}, and ω_{T3}) and one nonpolar vibration ω_4, which does not interact with photons.

c) Uniaxial diatomic crystals

In considering uniaxial diatomic crystals we have to decompose the vectors **w**, **E**, and **P** in Eq. (2.1) into two components:

$$\mathbf{w}=(w_\perp,\ w_\parallel),\ \mathbf{E}=(E_\perp,\ E_\parallel)\ \text{and}\ \mathbf{P}=(P_\perp,\ P_\parallel),$$

where the symbols $\perp$ and $\parallel$ denote the components of the vectors along directions perpendicular and parallel relative to the optic axis. In this case the solution of Eq. (2.14) can be divided into two parts, as described below.

1. When the vectors **w**, **E**, and **P** are perpendicular to the optic axis, we find that for any direction of the wave vector **k**:

$$\frac{k^2c^2}{\omega^2}=\varepsilon_\perp(\omega)=\varepsilon_{\perp\infty}+\frac{\varepsilon_{\perp0}-\varepsilon_{\perp\infty}}{\omega_{T\perp}^2-\omega^2}\omega_{T\perp}^2. \tag{2.18}$$

The modes corresponding to this solution were called by Loudon[72] the ordinary polaritons, by analogy with the ordinary photons whose refractive index is independent of the direction of photon propagation in a uniaxial crystal.

2. The second solution does not have such a simple relative configuration of the vectors **w**, **E**, and **P** relative to the optic axis and to the wave vector **k**. In this case the dispersion relationship is

$$\frac{k^2c^2}{\omega^2}=\frac{\varepsilon_\parallel(\omega)\,\varepsilon_\perp(\omega)}{\varepsilon_\parallel(\omega)\cos^2\alpha+\varepsilon_\perp(\omega)\sin^2\alpha}, \tag{2.19}$$

where $\varepsilon_\perp(\omega)$ is given by Eq. (2.18) and $\varepsilon_\parallel(\omega)$ is described by an analogous expression if the symbol $\perp$ is replaced by $\parallel$; α is the angle between the polariton wave vector **k** and the optic axis. It follows from Eq. (2.19) that in this case the polariton frequency depends not only on the wave vector but also on its direction relative to the optic axis of a crystal. The modes which arise in this case were called by Loudon[72] the extraordinary polaritons. It should be noted, that, for $\alpha=0$, Eq. (2.19) reduces to (2.18) and, consequently, in this case the dispersions of the extraordinary and ordinary polaritons are identical.

In analyzing the dispersion of polaritons in uniaxial crystals it is convenient to distinguish two limiting cases: 1) when the splitting between the frequencies of the longitudinal ω_L and transverse ω_T phonons (LO–TO splitting) due to the long-range electric fields predominates over the induced (by the lattice potential anisotropy) frequency splitting of the phonons polarized along the optic axis ($\omega_{T\parallel}$, $\omega_{L\parallel}$) and at right-angles to this axis ($\omega_{T\perp}$, $\omega_{L\perp}$); 2) the converse situation, when the anisotropy-induced splitting predominates over the LO–TO splitting. These limiting (as well as intermediate) cases are discussed in detail in Refs. 72 and 73. Therefore, we shall give only graphical illustrations (Figs. 3 and 4) of the results obtained in these two limiting cases.

It should be noted that the dispersion curves of the extraordinary polaritons intersect the horizontal lines corresponding to the longitudinal optical phonons (compare Figs. 3a and 3c with Fig. 4a). According to Lamprecht and Merten[74] such intersections can appear only if the polariton wave vector is directed along or at right-angles to the optic axis of a crystal. For an arbitrary direction of the polariton wave vector which is $\alpha\neq0$ and $\alpha\neq90°$, there cannot be such intersection

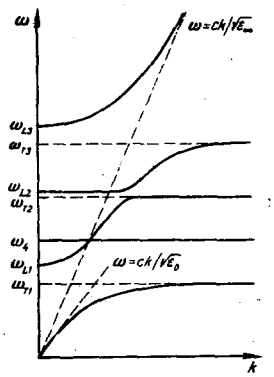

FIG. 2. Dispersion of polaritons in a cubic crystal with three polar and one nonpolar optical lattice vibrations.

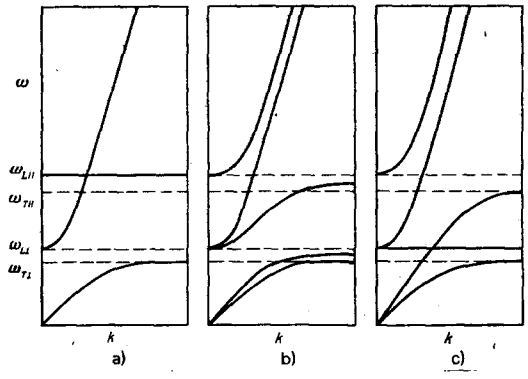

FIG. 3. Dispersion of polaritons in a diatomic uniaxial crystal in the case of predominance of the lattice potential anisotropy: a) $\alpha=0°$; b) $0°<\alpha<90°$; c) $\alpha=90°$.

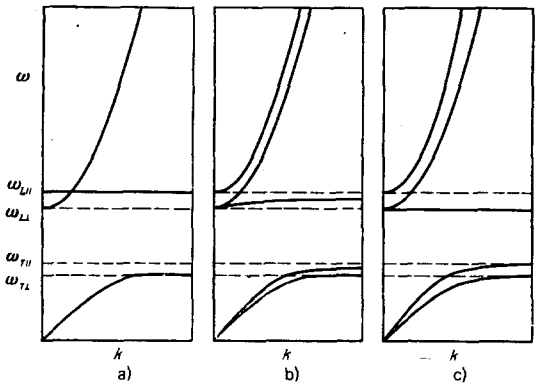

FIG. 4. Dispersion of polaritons in a diatomic uniaxial crystal in the case of predominance of the long-range electrostatic fields: a) $\alpha = 0°$; b) $0° < \alpha < 90°$; c) $\alpha = 90°$.

("anti-intersection of the dispersion branches"), as shown in Figs. 3b and 4b.

d) Biaxial polyatomic crystals

Merten[75] showed that the dispersion relationship for a polyatomic anisotropic crystal is given by the generalized Fresnel equation

$$\sum_{j=1}^{3} \frac{\hat{k}_j^2}{[\varepsilon(\omega)]^{-1} - [\varepsilon_j(\omega)]^{-1}} = 1, \tag{2.20}$$

which, together with the equation

$$\frac{k^2c^2}{\omega^2} = \varepsilon(\omega), \tag{2.21}$$

gives the polariton dispersion in a polyatomic anisotropic crystal. Here, $\hat{k}_j$ is the component of the unit vector $\mathbf{k}/k$ along the crystallographic axis x_j; $\varepsilon_j(\omega)$ is the dispersion relationship of the principal values of the permittivity,

$$\varepsilon_j(\omega) = \varepsilon_{j\infty} + \sum_{f}^{m_j} \frac{S_{jf}\omega_{jf}^2}{\omega_{jf}^2 - \omega^2}, \tag{2.22}$$

where $j = 1, 2, 3$; m_j is the number of the dipole-active lattice vibrations for which the vectors $\mathbf{w}$, $\mathbf{P}$, and $\mathbf{E}$ are directed along the crystallographic axis x_j; S_{jf} is the oscillator strength for a transition at the frequency of a transverse optical phonon ω_{jf}. Using the generalized LST relationship, we can rewrite the last expression in the form

$$\varepsilon_j(\omega) = \varepsilon_{j\infty} \prod_{f=1}^{m_j} \frac{\omega_{L,jf}^2 - \omega^2}{\omega_{jf}^2 - \omega^2}. \tag{2.23}$$

We note that when the polariton wave vector lies in one of the crystallographic planes, for example (x_i, x_j), the properties of the crystal resemble that of a uniaxial one. In this case the dispersion of the ordinary polaritons is given by

$$\frac{k^2c^2}{\omega^2} = \varepsilon_\gamma(\omega) \qquad (\gamma \neq i \neq j), \tag{2.24}$$

whereas the extraordinary polaritons are described by the dispersion relationship

$$\frac{k^2c^2}{\omega^2} = \frac{\varepsilon_i(\omega)\varepsilon_j(\omega)}{\varepsilon_i(\omega)\cos^2\alpha + \varepsilon_j(\omega)\sin^2\alpha}, \tag{2.25}$$

where α is the angle between the polariton wave vector $\mathbf{k}$ and the crystallographic axis x_i.

It thus follows that the polariton dispersion can be found if we know: a) the principal values of the permittivity $\varepsilon_{j\infty}$ in the transparency range; b) the frequencies of the transverse optical phonons ω_{jf}; c) the oscillator strengths S_{jf} at the frequencies ω_{jf} or the frequencies of the longitudinal optical phonons $\omega_{L,jf}$. The relationship between the sets of the parameters S_{jf}, ω_{jf} and ω_{jf}, $\omega_{L,jf}$ is described, for example, by the following expression:[86]

$$S_{jf} = \varepsilon_{\infty j} \frac{\omega_{L,jf}^2 - \omega_{jf}^2}{\omega_{jf}^2} \prod_{\beta \neq f}^{m_j} \frac{\omega_{L,j\beta}^2 - \omega_{jf}^2}{\omega_{j\beta}^2 - \omega_{jf}^2}. \tag{2.26}$$

3. FREQUENCY-ANGULAR SPECTRA OF RAMAN SCATTERING OF POLARITONS

The frequency-angular spectrum of the Raman scattering of light by polaritons, i.e., the dependence of the scattered-light frequency ω_s on the scattering angle φ, is governed by the laws of conservation of energy and momentum:[2)]

$$\left.\begin{aligned} \omega_l &= \omega_s + \omega, \\ \mathbf{k}_l &= \mathbf{k}_s + \mathbf{k}, \end{aligned}\right\} \tag{3.1}$$

where $\mathbf{k}_l$, $\mathbf{k}_s$, $\mathbf{k}$, ω_l, ω_s, and ω are the wave vectors and the frequencies of the exciting (laser) l and scattered s radiations and of the polaritons, respectively.

We shall begin by noting that the Raman scattering by polaritons in a crystal can be observed only in the simultaneous presence of dipole-active phonons (necessary for the appearance of polaritons) and Raman-active phonons. The optical phonons in noncentrosymmetric crystals have the necessary properties.

We shall now consider the problem of the scattering geometry in which the Raman scattering of light by polaritons can be observed. It is clear from Fig. 1 that the polariton frequency depends most strongly on the polariton wave vector for $k \sim k_{res}$. Usually the optical phonon frequency is $\omega_T \sim 10^{13}$ sec^{-1} and, consequently, $k_{res} = (\omega_T/c)\sqrt{\varepsilon_\infty} \sim 10^3$ cm^{-1}. The polariton wave vector observed in the "conventional" Raman scattering, i.e., when the scattering is observed at an angle of 90° relative to the direction of the exciting radiation, is of the same order of magnitude as the exciting photon vector, which is $k \sim \sqrt{2}k_l \sim 10^5$ cm^{-1} (Fig. 5). For these values of the wave vector the polariton frequency depends weakly on the wave vector and the scattering occurs effectively on phonons, i.e., in the range where the polariton nature of the dispersion of excitations is of little importance. Consequently, the scattering of light by polaritons (i.e., by excitations with $k \sim 10^3$ cm^{-1}) can be observed at small angles $\varphi \sim k/k_l \sim 10^{-2}$ rad (Fig. 5).

It follows that studies of the scattering of light by polaritons have to be carried out at small angles φ relative to the exciting radiation. A change in the scattering angle φ then also alters the wave vector $\mathbf{k}$ of the polaritons participating in the scattering process and, consequently, it alters the scattered-light frequency.

We shall now consider the frequency-angular spectrum of the Raman scattering by polaritons. We shall

[2)] For simplicity, in this section we shall consider only the Stokes scattering, i.e., we shall assume that $\omega_l > \omega_s$.

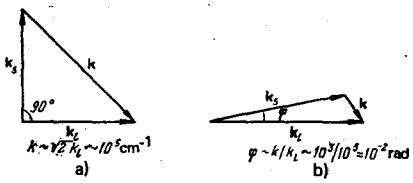

FIG. 5.

rewrite the condition (3.1) in the form

$$k^2(\omega) = k_l^2(\omega_l) + k_s^2(\omega_l - \omega) - 2k_l(\omega_l)\, k_s(\omega_l - \omega)\cos\varphi, \qquad (3.2)$$

where φ is the angle between the wave vectors of the exciting $\mathbf{k}_l$ and scattered $\mathbf{k}_s$ radiations. For clarity, we shall consider the frequency-angular spectrum in its graphical form. We can do this by plotting the polariton dispersion $k(\omega)$, as described in the preceding section. Next, the function

$$q(\omega) = \sqrt{\left| k_l^2(\omega_l) + k_s^2(\omega_l - \omega) - 2k_s(\omega_l - \omega)\, k_l(\omega_l)\cos\varphi \right|} \cdot$$
$$= \sqrt{\left| [k_l(\omega_l) - k_s(\omega_l - \omega)]^2 + 4k_l(\omega_l)\, k_s(\omega_l - \omega)\sin^2\frac{\varphi}{2} \right|} \qquad (3.3)$$

has to be plotted in the same graph for various fixed values of the angle φ. The intersection of the dispersion curves $k(\omega)$ with the curves representing $q(\omega)$ means that the Raman scattering of light by polaritons does take place and the ordinates of the points of intersection give the dependence of the frequency of the Stokes shift of the scattered radiation on the scattering angle φ.

The conditions $\omega_l \gg \omega$ and $\omega_s \gg \omega$ are usually satisfied in Raman scattering. If the frequencies ω_l and ω_s lie in the transparency range of a crystal, then $k_s(\omega_l - \omega)$ can be expanded as a series in ω and only the terms linear in ω need be retained. In this case, the expression (3.3) for cubic crystals can be rewritten in the form

$$q(\omega) = \sqrt{4k_l\left[k_l - \omega\left(\frac{\partial k}{\partial\omega}\right)_{\omega=\omega_l}\right]\sin^2\frac{\varphi}{2} + \left[\omega\left(\frac{\partial k}{\partial\omega}\right)_{\omega=\omega_l}\right]^2}. \qquad (3.4)$$

In practice it is usual to employ $\partial n/\partial\nu$ and ν ($\nu = \omega/2\pi c$) rather than $\partial k/\partial\omega$ and ω. In terms of the former quantities, Eq. (3.4) becomes

$$q(\nu) = 2\pi$$
$$\times \sqrt{\left[n_l + \nu_l\left(\frac{\partial n}{\partial\nu}\right)_{\nu=\nu_l}\right]^2\nu^2 + 4\nu_l(\nu_l - \nu)\, n_l\left[n_l - \nu_l\left(\frac{\partial n}{\partial\nu}\right)_{\nu=\nu_l}\right]\sin^2\frac{\varphi}{2}}. \qquad (3.5)$$

When light is scattered at small angles, we can also use the approximate expression $\sin^2(\varphi/2) \sim \varphi^2/4$.

Figure 6 illustrates a graphical method for the determination of the frequency-angular spectrum of the Raman scattering by polaritons in a cubic diatomic crystal of GaP. The continuous curves in Fig. 6 represent the polariton dispersion $k(\nu)$ of a GaP crystal calculated using Eq. (2.14b). The dashed curves are graphs of the function $q(\nu)$ for various fixed values of the angle φ and they are calculated from Eq. (3.5). The points of intersection of the continuous and dashed curves give the frequencies of the Stokes shifts for given scattering angles φ. The results of a graphical determination of the polariton frequencies and wave vectors corresponding to fixed scattering angles are given in Fig. 6 in the form of a table.

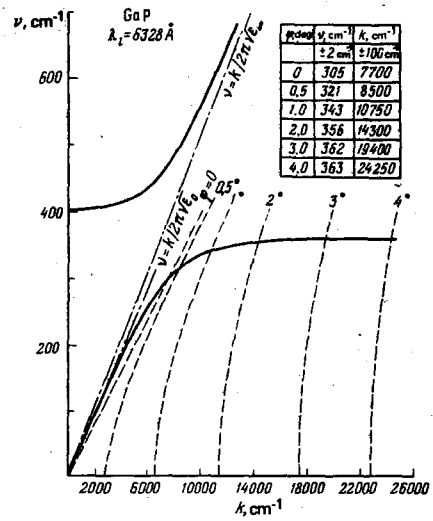

φ deg	ν, cm^{-1} ±2 cm^{-1}	k, cm^{-1} ±100 cm^{-1}
0	305	7700
0,5	321	8500
1,0	343	10750
2,0	356	14300
3,0	362	19400
4,0	363	24250

FIG. 6. Dispersion of polaritons (continuous curves) in a GaP crystal and graphs of the function $q(\nu) = |\mathbf{k}_l - \mathbf{k}_s|$ plotted for various values of the scattering angle φ (dashed curves).

The calculations were carried out using the following parameters of a GaP crystal:[76,77] $\nu_T = 367.3\ \mathrm{cm}^{-1}$, $\nu_L = 403.0\ \mathrm{cm}^{-1}$, $n_l = 3.315$ ($\lambda_l = 0.6328\ \mu$, $\nu_l = 15803\ \mathrm{cm}^{-1}$), $(\partial n/\partial\nu)_{\nu=\nu_l} = 0.422\times10^{-4}$ cm, $\varepsilon_\infty = 9.6$.

It is clear from Fig. 6 that the dashed curves do not intersect the upper dispersion branch of polaritons. This means that the scattering of light in a GaP crystal is impossible for polaritons belonging to the upper dispersion branch. This is true of any cubic crystal.[3)] In fact, the slope of the asymptote of the upper polariton branch, given by the expression $d\nu/dk = 1/2\pi\sqrt{\varepsilon_\infty}$, is less than the slope of the straight line $q(\nu)$ for $\varphi = 0$, given by the expression $d\nu/dq = 1/\{2\pi[n_l + \nu_l(\partial n/\partial\nu)_{\nu=\nu_l}]\}$.

Henry and Hopfield[1] were the first to observe experimentally the Raman scattering of light by polaritons in a GaP crystal; they used an He–Ne laser ($\lambda_l = 6328$ Å). Their experiment demonstrated clearly the dependence of the scattered-light frequency on the scattering angle and they found that the observed frequency-angular spectrum was in good agreement with the calculations.

a) Influence of exciting radiation wavelength

The frequencies of the polaritons participating in scattering depend not only on the scattering angle, as shown above, but also on the wavelength of the exciting radiation. This can be demonstrated by considering the scattering in exactly the forward direction ($\varphi = 0$) and assuming that the wavelength (frequency) of the exciting radiation is a variable quantity. In this case Eq. (3.5) can be written in the form

$$q(\nu, \nu_l) = 2\pi\nu\left[n_l(\nu_l) + \nu_l\left(\frac{\partial n}{\partial\nu}\right)_{\nu=\nu_l}\right]. \qquad (3.6)$$

[3)] This conclusion is valid if the frequencies ν_l and ν_l' are located within the normal dispersion region of a crystal. In principle, it is possible to observe the Raman scattering of light by polaritons of the upper branch in cubic crystals if the frequencies ν_l and ν_s lie in the anomalous dispersion region which is due to, for example, exciton of impurity resonances.

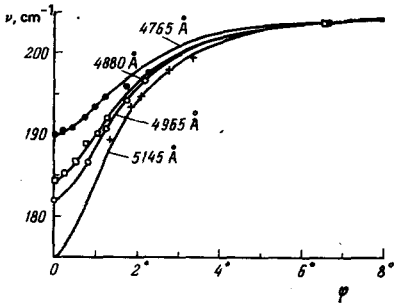

FIG. 7. Frequency-angular dependences of the scattering of light by polaritons in a cubic diatomic ZnSe crystal obtained at various exciting radiation wavelengths.[42]

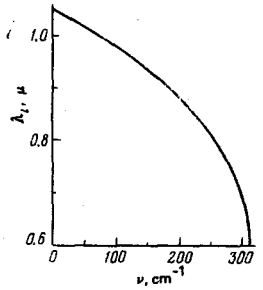

FIG. 8. Dependence of the frequency of polaritons active in the spectra of exact forward scattering ($\varphi = 0$) in a GaP crystal on the wavelength of the exciting radiation.

It is clear from this expression that a change in the wavelength (or frequency) of the exciting radiation alters the slope of the line $q(\nu)$ and, consequently, the coordinates of the intersection of this line with the dispersion branch of polaritons. This method of altering the frequency of the polaritons active in the scattering may be called the dispersion technique and a change in the frequency is manifested most clearly near the absorption region of a crystal, where n_l and $(\partial n/\partial \nu)_{\nu=\nu_l}$ increase rapidly as the value of ν_l is increased.[4)]

It should be noted that the slope of the line $q(\nu)$ decreases as the wavelength of the exciting radiation is increased and this is accompanied by a reduction in the Stokes shift in the forward scattering and, consequently, by a reduction in the range of tuning of the frequency of light Raman-scattered by polaritons by altering the scattering angle. It is possible to select the exciting radiation wavelength $\lambda_l = \lambda_l'$ ($\nu_l = \nu_l'$), given by

$$\sqrt{\varepsilon_0} = n_l(\nu_l') + \nu_l' \left(\frac{\partial n}{\partial \nu}\right)_{\nu=\nu_l'}, \tag{3.7}$$

for which $q(\nu)$ corresponding to $\varphi = 0$ coincides with the asymptote of the lower polariton branch and the lower polariton branch can be observed completely for the scattering of $\lambda_l \geq \lambda_l'$ wavelengths at small angles. Moreover, for $\lambda_l = \lambda_l'$ the condition (3.1) is obeyed immediately for a wide range of polariton frequencies in the lower dispersion branch, and this should broaden considerably the spectrum of light Raman-scattered by polaritons in the forward direction. However, this may turn out to be very useful in the coherent excitation of polaritons by two lasers because collinear excitation may provide a means for tuning the polariton frequency without altering the scattering geometry, i.e., it may provide frequency-insensitive phase matching for the excitation of polaritons in the lower dispersion branch.

The dependence of the frequency-angular polariton scattering spectra on the wavelength of the exciting radiation was first demonstrated experimentally for a cubic diatomic crystal of ZnSe (Ref. 41). Figure 7 shows the dependence of the Stokes shift on the scattering angle for the excitation with argon laser radiation of different wavelengths[42] (4765, 4880, 4965, and 5145 Å).

[4)]Near the absorption region of a crystal it is not always sufficient to take into account only the linear terms of the expansion $n_s(\nu_l - \nu)$ in powers of ν, as has been done in the derivation of Eq. (3.5).

The range of wavelengths used in the experimental studies of the excitation was in this case close to the absorption edge of the ZnSe crystal, where dispersion was strong and, in agreement with Eq. (3.6), this altered considerably the frequency-angular scattering spectra when the wavelength of the exciting radiation was varied.

Figure 8 shows, by way of example, the calculated dependence of the Stokes shift (or polariton frequency) of light scattered by polaritons in exactly forward direction on the wavelength of the exciting radiation incident on a GaP crystal. According to Eqs. (2.14) and (3.6), this dependence can be described by

$$n_l(\nu_l) + \nu_l \left(\frac{\partial n}{\partial \nu}\right)_{\nu=\nu_l} = \sqrt{\frac{\nu_0^2\varepsilon_0 - \nu^2\varepsilon_\infty}{\nu_0^2 - \nu^2}} = \sqrt{\varepsilon_\infty}\sqrt{\frac{\nu_L^2 - \nu^2}{\nu_T^2 - \nu^2}}. \tag{3.8}$$

The above expression was derived assuming the following parameters of a GaP crystal:[76] $\nu_T = 367.3$ cm^{-1}, $\nu_L = 403$ cm^{-1}, and $\varepsilon_\infty = 9.2$; the refractive index data were taken from Ref. 77.

It is clear from Fig. 8 that the frequency of the polaritons participating in the scattering depends strongly on the wavelength of the exciting radiation. The lower polariton branch may be observed completely in the experimental study of the scattering of light at small angles in the wavelength range $\lambda_l \gtrsim 1.05$ μ, whereas for $\lambda_l = 1.05$ μ the condition (3.7) is satisfied.

b) Frequency-angular spectra of anisotropic crystals

We shall start by considering the frequency-angular spectra of light scattered by polaritons in uniaxial crystals. We shall consider the specific example of a lithium iodate ($LiIO_3$) crystal and compare the main results also with the experimental data obtained for other crystals.

A crystal of $LiIO_3$ has two "molecules" in a unit cell and its space symmetry group[31] is $P6_3$ (C_6^6). Consequently, the total number of vibrations of the crystal lattice of lithium iodate is 30; they can be separated into the following irreducible representations:[70,31] $5A + 5B + 5E_1 + 5E_2$. The acoustic phonons are represented by the nondegenerate mode A and the doubly degenerate mode E_1. Thus, the remaining 27 optical vibrations can be described by the following irreducible representations: $4A + 5B + 4E_1 + 5E_2$. The Raman scattering tensor for crystals of the point symmetry group C_6, to which $LiIO_3$ belongs, has the form

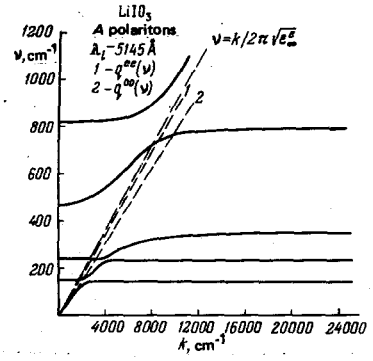

FIG. 9. Calculated dispersion curves of A polaritons (continuous curves) and graphs of the functions $q^{ee}(\nu)$ and $q^{oo}(\nu)$ (dashed lines 1 and 2) for an $LiIO_3$ crystal.

$$A(z)=\begin{pmatrix} a & 0 & 0\\ 0 & a & 0\\ 0 & 0 & b\end{pmatrix},\quad E_1(x)=\begin{pmatrix} 0 & 0 & c\\ 0 & 0 & d\\ c & d & 0\end{pmatrix},\quad E_1(y)=\begin{pmatrix} 0 & 0 & -d\\ 0 & 0 & c\\ -d & c & 0\end{pmatrix},$$
$$E_2=\begin{pmatrix} e & f & 0\\ f & -e & 0\\ 0 & 0 & 0\end{pmatrix},\quad E_2=\begin{pmatrix} f & -e & 0\\ -e & -f & 0\\ 0 & 0 & 0\end{pmatrix}. \qquad (3.9)$$

The B modes are inactive in the Raman and infrared spectra; the E_2 modes are Raman-active but infrared-inactive and, consequently, they do not interact with photons and do not transform into polaritons. The A and E_1 modes are Raman- and infrared-active so that they interact with photons and transform into polaritons that can appear in the low-angle Raman-scattering spectra.

The dispersion of the A and E_1 polaritons calculated from Eqs. (2.21) and (2.22) is represented by the continuous curves in Figs. 9 and 10, respectively; the calculations are carried out for the following parameters of $LiIO_3$ (Ref. 31): $\nu_{T,\parallel f}=148, 238, 358, 795\ cm^{-1}$; $S_{\parallel f}=0.0826, 0.0616, 2.30, 0.1406$; $\nu_{T,\perp f}=180, 330, 370, 769\ cm^{-1}$; $S_{\perp f}=0.1026, 1.672, 1.889, 0.625$; $\varepsilon_{\parallel\infty}=n^2_{e\infty}=3.06$; $\varepsilon_{\perp\infty}=n^2_{o\infty}=3.61$.

According to Eq. (3.9), the polarizations of the exciting and scattered radiation should be the same for light scattered by the A polaritons; consequently, in the case of exact forward scattering ($\varphi=0$), Eq. (3.3) should be

$$q^{oo}(\nu)=2\pi\nu\left[n_{lo}+\nu_l\left(\frac{\partial n_o}{\partial\nu}\right)_{\nu=\nu_l}\right] \qquad (3.10a)$$

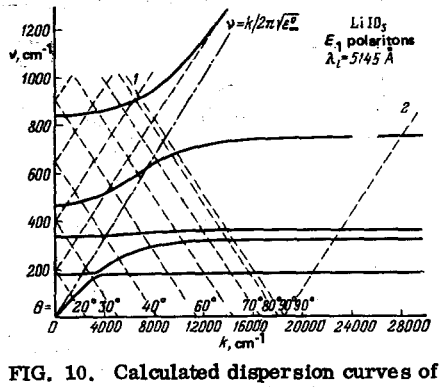

FIG. 10. Calculated dispersion curves of E_1 polaritons and graphs of the function $q^{eo}(\nu, \theta)$ for various angles θ (dashed curves) for an $LiIO_3$ crystal: 1) $q^{eo}(\nu, 90°)$; 2) $q^{oe}(\nu, 90°)$.

in the case when the exciting and scattered radiations are polarized ordinary (o) waves, and

$$q^{ee}(\nu)=2\pi\nu\left[n_{le}+\nu_l\left(\frac{\partial n_e}{\partial\nu}\right)_{\nu=\nu_l}\right] \qquad (3.10b)$$

when the exciting and scattered radiations are extraordinary (e) waves.[5)] Here, n_o is the ordinary and n_e is the extraordinary refractive index. The graphs of the functions $q^{oo}(\nu)$ and $q^{ee}(\nu)$ are represented by the dashed lines in Fig. 9. The refractive index data required in the calculations were taken from Ref. 79.

It is clear from Fig. 9 that the polaritons with smaller wave vectors are observed when the exciting and scattered radiations are polarized as the extraordinary waves, i.e., as the waves with the lower refractive indices ($n_o>n_e$ for $LiIO_3$). In this case the change in the frequency of the scattered radiation is greatest for small angles. This is discussed and demonstrated experimentally by Claus.[39]

However, it should be noted that in the geometries considered so far the scattering of light by polaritons of the upper dispersion branch is impossible in $LiIO_3$. But in general, the scattering of light by polaritons of the upper branch is sometimes possible in anisotropic crystals also when the polarization of the exciting and scattered radiation is the same. This requires that the following condition be satisfied:

$$\left[n_{l\alpha}+\nu_l\left(\frac{\partial n_\alpha}{\partial\nu}\right)_{\nu=\nu_l}\right]<\sqrt{\varepsilon_{\beta\infty}}\qquad(\alpha\neq\beta), \qquad (3.11)$$

where α and β define the directions of polarization of the exciting (and, consequently, of the scattered) radiation and of the polaritons, respectively. This condition may be satisfied in some crystals with a sufficiently strong birefringence, such as lithium formate, in which the scattering of light by the $A(z)$ polaritons of the upper dispersion branch has been observed for the scattering geometry $y(x, x)y+\Delta x$ (Ref. 80).

According to Eq. (3.9), the scattering of light by the E_1 polaritons is described by the nondiagonal Raman scattering tensor. Consequently, in the case of propagation of the exciting radiation at an angle of 90° to the optic axis of a crystal, the polarizations of the exciting and scattered radiations should be different. We can distinguish here two cases: in one case the exciting radiation is polarized as an ordinary wave and the scattered radiation as an extraordinary wave; in the other case the opposite is true. In the exact forward scattering ($\varphi=0$) the functions $q(\nu)$ corresponding to these two cases can be expressed in the form:

$$q^{oe}(\nu)=\left|2\pi\nu_l(n_{lo}-n_{le})+2\pi\nu\left[n_{le}+\nu_l\left(\frac{\partial n_e}{\partial\nu}\right)_{\nu=\nu_l}\right]\right|, \qquad (3.12a)$$

$$q^{eo}(\nu)=\left|2\pi\nu_l(n_{le}-n_{lo})+2\pi\nu\left[n_{lo}+\nu_l\left(\frac{\partial n_o}{\partial\nu}\right)_{\nu=\nu_l}\right]\right|, \qquad (3.12b)$$

[5)] The scattering geometry in the Raman spectroscopy is frequently denoted by $\alpha(\beta, \gamma)\delta$, where α and δ are the crystallographic axes along which the wave vectors of the exciting and scattered light are directed, whereas β and γ are the crystallographic axes along the directions of polarization of the exciting and scattered radiation, respectively. When light is scattered at small angles, the notation $\alpha(\beta, \gamma)\delta+\Delta\xi$ means also that for $\varphi\neq 0$ the scattered-radiation vector has a component along the crystallographic axis ξ.

respectively. The graphs of these functions are represented by the dashed lines in Fig. 10. It is clear from this figure that in the case of $LiIO_3$ (characterized by $n_0 > n_e$ and, consequently, $n_{1e} - n_{1o} < 0$) the magnitude of the polaritons participating in the forward scattering is smaller in the scattering geometry corresponding to the case (3.12b) than for the case (3.12a). This has been used[29,30] to obtain information on the dispersion of the E_1 polaritons in an $LiIO_3$ crystal in a wider range of the polariton frequencies and wave vectors. It should be pointed out that the same results were reported in the very first observations of the scattering of light by polaritons in uniaxial crystals.[2,11] Figure 11 shows, by way of example, the results of an experimental investigation of the Raman scattering of light by polaritons in a ZnO crystal (characterized by $n_o < n_e$) obtained for two different scattering geometries.[2]

It is worth noting the intersection of the dashed line 1 in Fig. 10 with the upper dispersion curve. This is a demonstration of the possibility of observing the scattering of light by polaritons of the upper branch. The intersection of the graphs of the function $q(\nu)$ with the upper polariton branch is generally possible at two points, as shown in Fig. 15. The scattering of light by high-frequency polaritons of the upper branch corresponds, in accordance with the established terminology, to the parametric scattering mentioned in the Introduction.

We shall consider another possibility of using birefringence of crystals in studies of the scattering of light by polaritons. In an anisotropic crystal the wave vector of the extraordinary wave is a function of the direction of propagation or of the angle θ between the wave vector of the light wave and the optic axis of the crystal. Therefore, for an arbitrary direction of the exciting radiation with the extraordinary polarization the expression for $q^{eo}(\nu)$ in the direction $\varphi = 0$ can be written in the form

$$q^{eo}(\nu) = \left| 2\pi\nu_l [n_{1e}(\theta) - n_{1o}] + 2\pi\nu \left[n_{1o} + \nu_l \left(\frac{\partial n_o}{\partial \nu} \right)_{\nu=\nu_l} \right] \right|, \qquad (3.13)$$

where

$$n_{1e}(\theta) = \frac{n_{1o} n_{1e}}{\sqrt{n_{1o}^2 \sin^2\theta + n_{1e}^2 \cos^2\theta}}.$$

It is clear from Eq. (3.13) that the function $q^{eo}(\nu, \theta)$ depends on the angle θ and, consequently, the coordinates of the intersections of a graph of this function with the dispersion curves of polaritons also depend on the angle θ (Fig. 10). This means that the frequency of light scattered by polaritons can be altered by changing the direction of the exciting radiation relative to the optic axis of a crystal while keeping the scattering angle fixed. This possibility was first demonstrated by Dobrzhanskiĭ *et al.*[34]

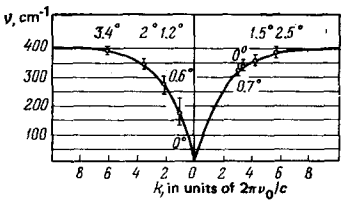

FIG. 11. Calculated dispersion curves of polaritons of the lower branch of a diatomic uniaxial ZnO crystal and experimental values (circles)[2] obtained by the scattering of light at low angles in the following geometries: a) $x(y, z)x + \Delta z$; b) $x(z, y)x + \Delta z$. The scattering angles are given above the circles.

It is also clear from Fig. 10 that for an $LiIO_3$ crystal we can find the optimal angle $\theta = \theta_{opt}$ for which the wave vector of a polariton from a given dispersion branch participating in scattering is zero, i.e., we can ensure that the intersection between the dispersion curve and the dashed line occurs at $k = 0$. In this case a study of the low-angle Raman scattering of light by polaritons for $\theta = \theta_{opt}$ makes it possible to find the dispersion of polaritons in the selected branch with wave vectors from $k \sim 10^5$ cm^{-1} to $k = 0$. The value of θ_{opt} can be calculated from

$$k(\theta_{j\,opt}) = 2\pi\nu_l [n_{1e}(\theta_{j\,opt}) - n_{1o}] + 2\pi\nu_{L,\,j-1} \left[n_{1o} + \nu_l \left(\frac{\partial n_o}{\partial \nu} \right)_{\nu=\nu_l} \right] = 0, \qquad (3.14)$$

where $\nu_{L,j-1}$ is the frequency of the $(j-1)$-th longitudinal optical phonon. The solution of Eq. (3.14) for $j = 1$ ($\nu_{L,0} = 0$ and $\theta_{1\,opt} = 0°$) is valid on condition that $[n_{1o} + \nu_l (\partial n_0 / \partial \nu)_{\nu=\nu_l}] \leqslant \sqrt{\varepsilon_\perp(0)}$. A calculation of $\theta_{j\,opt}$ for the E_1 polaritons in an $LiIO_3$ crystal gives $\theta_{1\,opt} = 0°$, $\theta_{2\,opt} = 19.5°$, $\theta_{3\,opt} = 25°$, $\theta_{4\,opt} = 32.5°$, and $\theta_{5\,opt} = 48°$, where $\theta_{5\,opt}$ corresponds to the optimal angle for the upper polariton branch.[37] An experimental investigation of the low-angle scattering of light by the E_1 polaritons in an $LiIO_3$ crystal for $\theta_{4\,opt} = 32.5°$ has made it possible to find, for example, the polariton dispersion in the range of wave vectors from $k = 2 \times 10^5$ cm^{-1} to $k = 0$ for the 460–769 cm^{-1} branch. The results of this investigation are presented in Fig. 12. The scattering of light in the $\theta = 90°$ case is possible only for polaritons lying to the right of the dashed line.

We have considered above the possibility of varying the scattered-light frequency by altering the direction of propagation of the exciting radiation (rotation of the crystal) in the case of anisotropic crystals when the exciting radiation has the extraordinary polarization and the scattered radiation and polaritons have the ordinary polarization. This frequency tuning method is operative whenever one of the three waves participating in the scattering process is extraordinary. For example, the case of tuning the scattered-light frequency by altering the direction of the wave vector of the extraordinary

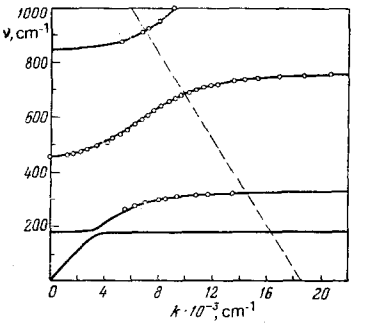

FIG. 12. Dispersion of E_1 polaritons in an $LiIO_3$ crystal (the experimental data represented by circles) obtained for $\theta_{opt} = 32.5°$ and reported in Ref. 37.

polaritons is considered in Ref. 32.

It should be pointed out that the intensity of the light scattered by the extraordinary (oblique or mixed $E_1 + A$) polaritons differs from zero for the extraordinary polarization of the exciting radiation and the ordinary polarization of the scattered wave if $\varphi \neq 0$ and the scattering plane does not coincide with the crystallographic plane (x, y). In this case the polariton frequency depends not only on the magnitude but also on the direction of the polariton wave vector. When the scattering plane is, for example, perpendicular to the (x, z) plane, the direction of the polariton wave vector is given by

$$\cos\alpha = \frac{k_l - k_s\cos\varphi}{k}\cos\theta. \qquad (3.15)$$

The experimental frequency-angular spectra can be used to determine all the quantities on the right-hand side of the above expression. Moreover, if we know the dispersion of the E_1 polaritons, which can be measured—for example—in the scattering geometry described above, we can then calculate also the dispersion of the A polaritons employing the relationship

$$k_A^2(\nu) = \frac{[k(\nu)]^2[k_E(\nu)]^2\sin^2\alpha(\nu)}{[k_E(\nu)]^2 - [k(\nu)]^2\cos^2\alpha(\nu)}. \qquad (3.16)$$

In the case of $LiIO_3$ crystals this method has yielded the dispersion of the upper branch of the A polaritons and has made it possible to study the range of small polariton wave vectors of the lower branches.[37]

Moreover, if the scattering plane lies in the (x, z) plane, then the frequency-angular spectrum of the scattering of light by the extraordinary polaritons is generally asymmetric relative to the sign of the angle φ if $\theta \neq 0$ and $\theta \neq 90°$. In this case the dispersion of the E_1 and A polaritons can be found in a single operation from the asymmetry of their frequency-angular spectra.[37]

An analysis of these spectra can be easily applied also to biaxial crystals. In this case the dependence of the refractive indices is governed by the Fresnel equation[82] and the dependence of the polariton frequency on the magnitude and direction of the wave vector is described by the generalized Fresnel equation (2.20).

In addition to these methods for altering the polariton frequency, one should also mention the influence of the temperature of the crystal and of an external electric field. The effect of a change in the temperature of the crystal on the frequency-angular scattering spectra can be allowed for by introducing the temperature dependence of the refractive index into the relevant expression of the type of Eq. (3.2). Such an influence has been especially widely investigated in studies of the parametric scattering of light [83,139] and at present the temperature dependence of the frequency of the scattered radiation is being used successfully in some optical parametric oscillators.[83,139] The polariton dispersion usually depends weakly on temperature, with the exception of polaritons associated with the soft modes of ferroelectric crystals,[84] whose frequency tends to zero as the phase transition temperature is approached.

The application of an external electric field to a crystal alters the refractive indices because of the electrooptic effect.[85] Allowance for the scattering geometry and the symmetry of a crystal makes it possible to find the explicit dependence of the refractive index on an external electric field and thus allow for the influence of this field on the frequency-angular scattering spectra. The use of the electrooptic effect to alter the frequency of the scattered light has been demonstrated in parametric generation of light.[83] Usually this effect is weak but in ferroelectric crystals it may increase by more than two orders of magnitude on approach to the Curie temperature.[85,89] This has been used to achieve considerable electrooptic tuning of wavelengths in an optical parametric oscillator utilizing a KDP crystal.[90,91] However, this effect has not been observed in the polariton part of the scattered-light spectrum.

We shall conclude by listing the methods that can be used to alter (tune) the frequency of light scattered by polaritons: a) variation of the scattering angle, which is the most widely used, effective, and universal method; b) variation of the wavelength of the exciting radiation (dispersion method); c) variation of the direction of the exciting radiation in a crystal (rotation of a crystal) in a fixed scattering geometry, which can be used only in the case of anisotropic crystals when at least one of the three excitations participating in the scattering process has the extraordinary polarization; d) variation of the temperature of a crystal; e) application of an external electric field.

c) Frequency-angular spectra in the case of polariton attenuation

We have discussed so far the frequency-angular spectrum of the scattered light ignoring polariton attenuation. However, we have to consider the effect of such attenuation.

If the frequencies of the exciting and scattered light are within the transparency range of a crystal, all the quantities in Eq. (3.1) are real. In view of this, an attempt has been made[13] to relate ω and k at the maximum of a Raman line obtained for a given scattering angle and the expression suggested is $c^2k^2/\omega^2 = n^2$, whereas other authors[92] used $c^2k^2/\omega^2 = \varepsilon'$, where

$$\frac{c^2k^2}{\omega^2} \equiv (n + i\varkappa)^2 = \varepsilon(\omega) = \varepsilon'(\omega) + i\varepsilon''(\omega). \qquad (3.17)$$

In both cases ω and k are real and, therefore, attempts have been made to replace the complex quantity $\varepsilon(\omega)$ in Eq. (3.17) by the real values of n^2 or ε'. However, such a replacement is not justified in any way and it does not produce results that agree with experiment. In fact, in this case the dispersion curve of polaritons acquires a turning point (such as that shown as a dashed curve in Fig. 13) at some critical value $k = k_{cr}$, which means that there is no Raman scattering at high scattering angles.

The problem is that the dispersion relationship (3.17) links ω with k only for solutions of homogeneous field equations. In the presence of absorption the relationship between ω and k naturally becomes complex. In the scattering of light we are dealing with the solutions of inhomogeneous field equations and then ω and k in Eq. (3.1) are the frequency and wave vector of a driving force and, in general, there is no dispersion relationship between ω and k. However, if we ignore absorp-

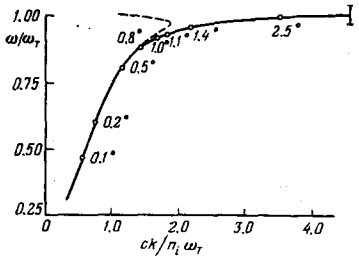

FIG. 13. Dispersion of polaritons in a ZnSe crystal. Calculations carried out using $c^2k^2/\omega^2 = \varepsilon'(\omega)$ with the attenuation constant $\Gamma = 7.5$ cm^{-1} (dashed curve) and also using Eq. (2.14a) (continuous curve); circles represent the results of a numerical calculation of the position of the center of the scattering line allowing for the attenuation and assuming various values of the scattering angle φ (Ref. 92).

tion, the scattering cross section is a δ function, i.e., the scattering intensity is high only under exact resonance conditions. Therefore, in a scattering line the values of ω and k are related in the same way as in the case of attenuation-free polaritons. However, in the presence of absorption under steady-state conditions the incident field excites the scattered field and forced vibrations in a medium and then the frequency and wave vector of these waves ω and k are generally not equal to the frequency and wave vector of normal waves.

In view of this situation the dependence $\omega(k)$ which appears in the frequency-angular scattering spectrum should be determined from the center of the scattering line obtained by calculating the Raman scattering cross section allowing for attenuation in the equations of motion of the crystal lattice. The results of such calculations[92-94] show that the dependences $\omega(k)$ correspond accurately to the dispersion relations in the absence of absorption, i.e., they correspond to the relationships obtained in Sec. 2. Figure 13 shows, by way of example, the polariton dispersion for a ZnSe crystal[92] obtained from the relationships $c^2k^2/\omega^2 = \varepsilon'(\omega)$ for $\Gamma = 7.5$ cm^{-1} (dashed curve), the dispersion calculated from Eq. (2.14a) (continuous curve), and that deduced from a numerical calculation based on the center of the scattering line (points). Thus, even in the case of sufficiently strong absorption of normal waves, the frequency-angular scattering spectrum governs (or is governed by) the dispersion relationship of polaritons which would have traveled in a given medium in the absence of absorption.

In the present section we have analyzed the frequency-angular scattering spectra assuming certain types of polariton dispersion. In practice, we meet usually the converse problem of determination of the polariton dispersion from the experimentally obtained frequency-angular scattering spectra. However, the above analysis of the principal features of possible frequency-angular spectra of the scattering of light by polaritons makes it possible to select experimental conditions in such a way as to obtain the required information.[6)]

[6)]A discussion of some of the problems touched upon in Sections 2 and 3 can be found in Refs. 9, 161, and 162.

4. EXPERIMENTAL METHODS FOR INVESTIGATING RAMAN SCATTERING BY POLARITONS

As shown in the preceding section, Raman scattering of light by polaritons can be observed at small angles relative to the direction of the exciting radiation. The greatest interest lies in the scattering of light within the angular range from 0° to 2°–10°, depending on the actual crystal. It follows that the exciting radiation should be characterized by a small divergence and a sufficiently high spectral brightness. These requirements are satisfied by laser radiation. This is why the scattering of light by polaritons was first observed only after the appearance of lasers.[1,2]

In studies of the scattering of light at low angles it is usual to employ either the photographic or the photoelectric method. The photographic method gives directly the dependence of the scattered-light frequency on the scattering angle over a wide spectral range. The method gives extensive information and is sufficiently accurate for the determination of the frequencies and scattering angles. However, when measurements are made of the scattered-light intensities, it is preferable to use the photoelectric method. The two methods are complementary and used together can give us full information on the scattering of light by polaritons.

a) Photographic method

The photographic method was first used to study the low-angle parametric scattering of light, i.e., the Raman scattering of light by polaritons of the "photon" part of the upper dispersion curve in the case of noncollinear propagation of light waves.[95] This method has been improved later[14,37] and it can be used at present to study the scattering of light by polaritons including those belonging to the lowest-frequency dispersion branch.[39]

In the photographic method the slit of a spectrograph is set with high accuracy in the focal plane of a lens located beyond the crystal being investigated on the same axis as the laser beam. Then, different scattering angles are focused at different points along the height of the slit, so that a given point collects the scattered light traveling only at some specific angle relative to the direction of the exciting radiation (Fig. 14). The midpoint of the slit then corresponds to the exact forward scattering. Consequently, a photographic film recorded by such a spectrograph when its slit is illuminated as above records a two-dimensional spectrogram representing the dependence of the scattered-light fre-

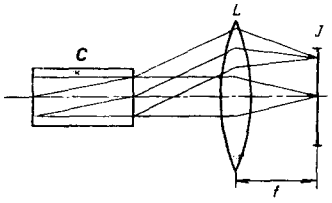

FIG. 14. Formation of the angular spectrum of scattered light on a spectrograph slit J. Here, C is the investigated crystal and L is an objective located at the focal length from the spectrograph slit.

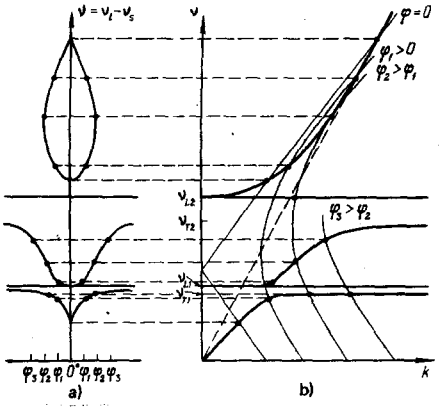

FIG. 15. Graphical method for determination of frequency-angular scattering spectra obtained by photographic recording method.

quency on the scattering angle. The distance h from the center of the slit to some point along its height is in one-to-one correspondence with the scattering angle φ' measured outside the crystal and in the approximation of low scattering angles this relationship is[7)]

$$\varphi' = \frac{h}{f}, \tag{4.1}$$

where f is the focal length of the lens. Figure 15a shows the frequency-angular scattering spectrum obtained by the photographic method for a crystal whose polariton dispersion is shown in Fig. 15b.

The necessary linear dimensions of the angular scan of the spectrum can be obtained and vignetting by various parts of a spectrograph can be avoided if a telescope is placed between a crystal and a lens. If f_1 and f_2 are the focal lengths of the first and second (counting from the crystal) telescope lenses, Eq. (4.1) becomes

$$\varphi' = \frac{f_2}{f_1}\frac{h}{f}. \tag{4.2}$$

Thus, the angular scale of the spectrum can be varied by altering the focal lengths of the telescope lenses. It should be pointed out that in determining the angular scale of this spectrum from a photographic film it is necessary to allow also for the magnification of the spectrograph.

The angular scale can be calibrated also on the basis of the angular spectrum of a Fabry–Perot interferometer placed in the same position as the crystal being investigated and illuminated with, for example, light from a mercury lamp. The radiation corresponding to some specific interference order emerges from the interferometer at a fixed angle relative to the optic axis of the system, so that a set of rings forms on the spectrograph slit and the diameters of these rings are in one-to-one correspondence with the angles associated with different interference orders. Thus, the spectral lines of mercury emerging from the spectrograph are "cut" by horizontal lines separated by a linear distance, which is in one-to-one correspondence with the angular

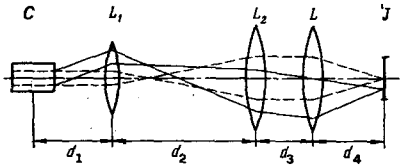

FIG. 16. Example of an optical system used in photographic recording of frequency-angular scattering spectra. Here, C is the investigated crystal; L_1, L_2, and L are objectives with focal lengths 94, 300, and 50 mm, J is a spectrograph slit; $d_1 \approx 110$ mm, $d_2 = f_1 + f_2 = 394$ mm, $d_3 \approx 50$ mm, and $d_4 = 50$ mm.

distance between the interference orders.

Correct illumination of a spectrograph is obtained when the following conditions are satisfied: a) the radiation scattered at the largest required angle φ'_{max} should not escape beyond the aperture of the exciting radiation beam over the whole length of a crystal l, i.e., $l\varphi_{max} \lesssim w$, where w is the diameter of the exciting radiation beam; b) the radiation scattered at an angle φ'_{max} should not escape outside the "working" height of the spectrograph slit, i.e., the condition $\varphi'_{max} f \lesssim h_0$ should be satisfied, where h_0 is the half-height of this working part of the slit, or one should ensure that $\varphi'_{max} f f_1/f_2 \lesssim h_0$ if a telescope is used; c) the scattered radiation should not escape outside the angular aperture of the spectrograph, i.e., $2\varphi_{max} f \lesssim RA$, where RA is the relative aperture of the spectrograph.

Figure 16 shows, by way of example, a specific system used to illuminate the slit of an ISP-51 spectrograph in investigations of the frequency-angular spectra of the scattering of light at low angles used by the present author. This system makes it possible to record these spectra in the range of angles φ' from 0° to about ±12°.

The most suitable cw laser for the excitation of the light-scattering spectra in the photographic method is the argon ion laser emitting in the blue-green part of the spectrum. The radiation power at the strongest emission wavelengths 4880 Å and 5145 Å exceeds 1 W and the frequency-angular spectrum of the scattered light obtained using these lines lies within the range of relatively high sensitivity of photographic materials.

The main difficulty in the photographic method is the selection of an optical filter which has to attenuate the laser radiation by several orders of magnitude so as to avoid overexposing the photographic film with the exciting radiation, and which has to transmit the scattered light producing the smallest possible Stokes shift. The required attenuation can be achieved using a Glan prism with a polished side face for removing the exciting radiation and additional optical filters (ZhS-18 for the exciting radiation of the 4880 Å wavelength, OS-11 for 5145 Å, and ZhS-17 for 4765 Å). However, the scattered radiation should be polarized perpendicularly to the laser radiation.[14,21,22,55]

In some experiments (see, for example, Refs. 7, 37, 54, and 56) the laser radiation has been attenuated by a CdS crystal with a sharp absorption edge, in which luminescence is generated in the infrared part of the spectrum where photographic films have a very low sensi-

[7)] The angle φ, measured inside the crystal, is—in this approximation—related to φ' by $\varphi \approx \varphi'/n_s$, where n_s is the refractive index for the scattered light.

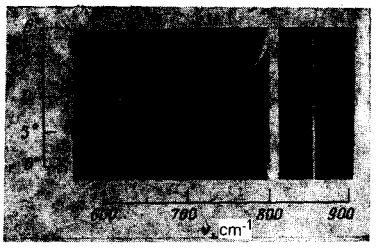

FIG. 17. Frequency-angular spectrum of the scattering of light by polaritons of one of the dispersion branches of a cubic $NaBrO_3$ crystal. The spectrum was recorded with an STÉ-1 spectrograph and excited with argon laser radiation of 5145 Å wavelength; the angle φ was measured inside the crystal.

tivity. The use of CdS crystals in combination with an argon laser emitting at 5145 Å wavelength has made it possible to record the scattered spectra with a Stokes shift from 400 cm^{-1} or higher without the use of Glan prism. Cooling of CdS to a temperature of the order of −30°C makes it possible to extend the measurements to 100 cm^{-1}. Figures 17 and 18 show the frequency-angular spectra of light scattered at small angles in some crystals using an argon laser (5145 Å, 1 W) and a CdS crystal as a filter.

The use of an iodine filter is very promising for the attenuation of the exciting radiation. Iodine vapor is characterized by a strong absroption line at the wavelength of 5145.42 Å, which lies in the stimulated emission range of the argon lasers. An argon laser operated in the multimode regime generates a spectrum about 8 GHz wide centered on the wavelength of 5145.36 Å. The use of a Fabry–Perot etalon makes it possible to ensure single-frequency emission with a line about 8 MHz wide which can then be tuned by, for example, rotation of the etalon to the absorption line of iodine whose width at 80°C is of the order of 300 MHz. Use of a filter in the form of an iodine cell 10 cm long kept at a temperature of 80–100°C has made it possible[39] to obtain the frequency-angular spectra of the light scattered by polaritons of the lower dispersion branch of $LiIO_3$ in the

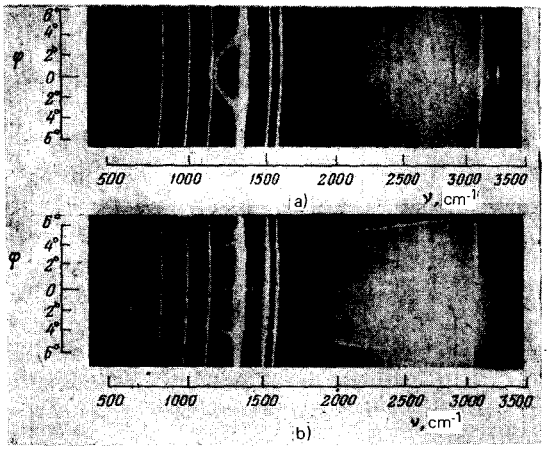

FIG. 18. Frequency-angular spectrum of the scattering of light in a crystal of metadinitrobenzene obtained with an ISP-51 spectrograph:[61] a) scattering geometry $x(z,\ z+y)x+\Delta z$; b) exciting radiation traveling and polarized in the $(x,\ z)$ plane at 45° relative to the x and z axes; scattering plane $(x,\ z)$.

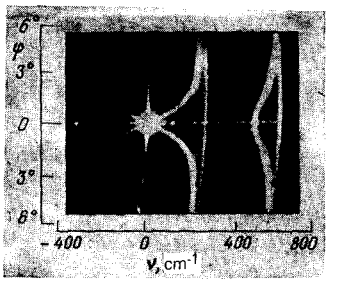

FIG. 19. Frequency-angular spectrum of the scattering of light by polaritons in an $LiNbO_3$ crystal. An iodine filter was used to attenuate the 5145 Å line of the exciting radiation. The scattering geometry was $y(z,\ z+x)y+\Delta x$. The exposure time was 2 min.

Stokes and anti-Stokes parts of the spectrum with shifts up to 15 cm^{-1}, which is not the smallest attainable value. The frequency-angular spectra of light scattered by $LiNbO_3$ and $LiIO_3$ crystals obtained using an iodine filter are shown in Figs. 19 and 20.

The use of image amplifiers is a convenient complement to the photographic method. It is then possible to excite the scattering spectra with lasers emitting red and near-infrared radiation, which extends considerably the capabilities of the photographic method and the range of crystals that can be employed, including semiconductors with fairly narrow band gaps. For example, the possibility of recording the scattering spectra excited by ruby laser radiation (6943 Å) is reported in Ref. 105. The laser was operated in the free-oscillation regime at a repetition frequency of 12.5 Hz. The spectra are recorded with a three-stage image amplifier which has an oxygen–cesium photocathode. The exciting radiation is attenuated by a cooled CdSe crystal, which makes it possible to record the scattered radiation with a shift of 90 cm^{-1} or more. Gating of an image amplifier in such a system can increase considerably the sig-

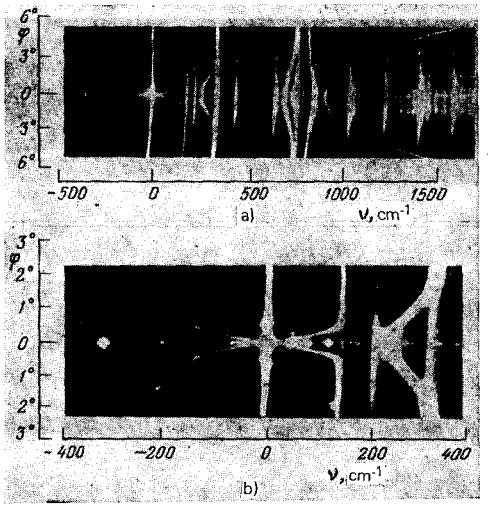

FIG. 20. Frequency-angular spectra of the scattering of light in an $LiIO_3$ crystal. An iodine filter was used to attenuate the exciting radiation.[39] The scattering geometries were $x(z,\ z+y)x+\Delta z$ (a) and $x(z,\ z+y)x+\Delta y$ (b). The exposure time was about 10 min. Asterisks are used to identify the luminescence line of the iodine filter.

nal/noise ratio and make it possible, in principle, to record fairly weak signals down to a few photoelectrons per image element.

b) Photoelectric method

In the photoelectric method it is usual to employ a spectrometer with an optical system for collecting the scattered light in a small solid angle oriented in some definite way relative to the exciting radiation beam. Repeated recording of the spectrum for different fixed scattering angles makes it possible to determine the dependence of the scattered-light frequency on the scattering angle (frequency-angular scattering spectrum).

In cubic crystals the scattered photons corresponding to different polaritons are emitted in a cone whose axis coincides with the direction of the exciting radiation. Consequently, the most effective collection of the scattered light is obtained by the use of circular screens located around the direction of the incident laser beam, as shown in Fig. 21 (Ref. 106). This makes it possible to record the light scattered along directions bounded by two cones with vertex angles $2\varphi'$ and $2(\varphi'+\Delta\varphi')$. Reduction in $\Delta\varphi'$ makes it possible to determine more accurately the wave vector participating in the polariton scattering and an increase in $\Delta\varphi'$ makes it possible to enchance the intensity. Thus, in each specific case it is possible to find the most suitable value of $\Delta\varphi'$ depending on the material and dimensions of the sample, laser output power, and characteristics of the electronic recording system. The finite nature of $\Delta\varphi'$, which makes it possible to record simultaneously polaritons corresponding to different wave vectors, broadens the observed Raman scattering lines and this is manifested most strongly in that part of the k space where the dispersion is high. The finite nature of $\Delta\varphi'$ is due to two factors: the finite width of a slit in the screen (see Fig. 21a) and the length of the crystal along the direction of the exciting radiation (Fig. 21b). The influence of the latter factor can be reduced only by increasing the focal length of the objective L or by reducing the thickness of the sample.

This observation method is most effective in the case of cubic crystals when the anisotropy can be ignored. The only shortcoming of this method is associated with the fact that the geometry of illumination of the spectrometer varies somewhat with the scattering angle. For small angles φ' the central part of the diffraction grating is illuminated more strongly, whereas for larger

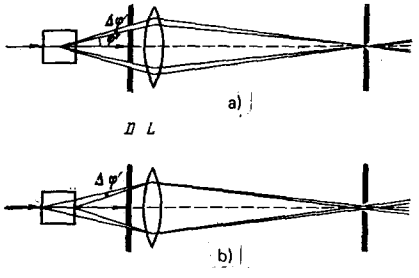

FIG. 21. Influence on the value of $\Delta\varphi'$ (a) of the finite slit width in the screen D and (b) of the finite length of the sample in the direction of the optical axis of the system.

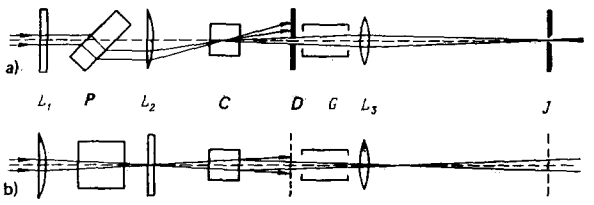

FIG. 22. Method of illumination of spectrometer slit in observation of the scattering of light at low angles in anisotropic crystals: a) vertical projection; b) horizontal projection.

angles the edges of the grating receive more light. This has to be allowed for in the determination of the scattered-light intensity.

In uniaxial crystals the frequency of the extraordinary polaritons depends not only on the polariton wave vector but also on the angle between its direction and the optical axis of the crystal. However, in the range of low scattering angles the direction of the polariton wave vector depends strongly on the value of φ so that the above method cannot give unambiguous spectra although it can be used sometimes to study the scattering of light by the ordinary polaritons in uniaxial crystals.

The optical system for investigating the scattering of light by the extraordinary polaritons is shown in Fig. 22 (Ref. 106). A parallel beam of laser radiation enters the system from the left. A cylindrical lens L_1 with a horizontal axis transforms this parallel beam into a fan of rays in the vertical plane. A thick glass plate P displaces the fan-shaped beam, parallel to itself, in the horizontal plane. Rotation of the plate P can alter the displacement. A second cylindrical lens L_2, whose axis is vertical, deflects the displaced beam toward the optical axis of the system and focuses the beam as a vertical strip on this axis. The position of the point of intersection of the beam with the axis is independent of the horizontal displacement of the beam by the plate P. A scattering crystal C is placed at this point. The radiation scattered at an angle φ' is selected by a slit D and reaches an objective L_3, which projects the scattering region onto the vertical slit J of a spectrometer. The image of the scattering region is a vertical strip, which can easily be made to coincide with the slit J. The whole system is designed so that the height of the exciting radiation beam does not exceed the height of the sample and the height of the image of the scattering region in the plane of the slit J does not exceed the height of the slit.

The scattered radiation is recorded at an angle φ' governed by the horizontal displacement of the beam at the entry to the lens L_2. For $\varphi' \neq 0$ the exciting radiation cannot pass through the split D and, therefore, any polarizer can be placed in front of the slit J to analyze the scattered radiation. It is important to note that in this system the conditions for illumination of the spectrometer monochromator are independent of the scattering angle φ'.

In view of the fact that the heights of the slits D and J are finite, the radiation scattered through an angle φ' in the horizontal plane and through various angles in the vertical plane is recorded simultaneously. The associ-

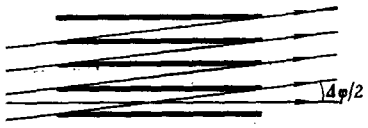

FIG. 23. Soller collimator limiting the divergence of recorded radiation in the vertical plane.

ated broadening of the Raman scattering lines can be reduced by introducing a Soller collimator G, through which rays pass as shown in Fig. 23. The horizontal slits of this collimator limit the divergence of the recorded radiation in the vertical plane to angles inclined at $\pm\Delta\varphi/2$ relative to the optical axis.

Some modifications of this photoelectric method are described in Refs. 17 and 118, and the theory of the instrumental distortions in photoelectric measurements of the polariton scattering lines is considered in Ref. 107. It should be noted that the slit of the monochromator can be illuminated in the photoelectric method in the same way as the slit of a spectrograph in the photographic method. However, one needs an additional stop (diaphragm) at the entry or exit slit of the monochromator so as to select a restricted region along the slit height. The dimensions of the aperture in such a stop govern the angle $\Delta\varphi'$.

Figures 24 and 25 show, by way of example, the spectra of light scattered by polaritons in $LiIO_3$ and SiO_2 crystals obtained for various scattering angles φ by the photoelectric method.

5. INTENSITY OF RAMAN SCATTERING BY POLARITONS

From the quantum point of view the process of spontaneous Raman scattering of light by polaritons can be regarded as the "decay" of an exciting radiation photon $\hbar\omega_l$ into two quanta: a Stokes quantum $\hbar\omega_s$ and a polariton $\hbar\omega$. Therefore, the probability of this decay is calculated in the third order of perturbation theory using $\hat{\mathcal{H}}' = -\int \hat{\mathbf{P}}\cdot\hat{\mathbf{E}}\,dv$, where $\hat{\mathbf{P}}$ is the operator representing the specific polarization of a crystal and $\hat{\mathbf{E}}$ is the electric field operator of an electromagnetic wave in the crystal; this probability is given by the expression

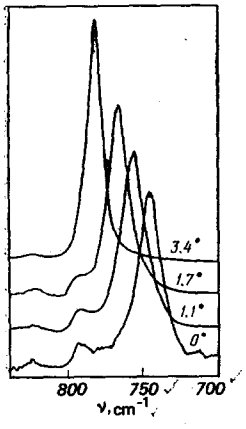

FIG. 24. Spectra of light scattered by polaritons corresponding to A phonons with $\nu_{TO}=795$ cm^{-1} in an $LiIO_3$ crystal, recorded for different scattering angles φ (Ref. 9). Exciting radiation wavelength 5145 Å, $\Delta\varphi'=0.5°$, scattering geometry $x(z,\ z)x+\Delta y$.

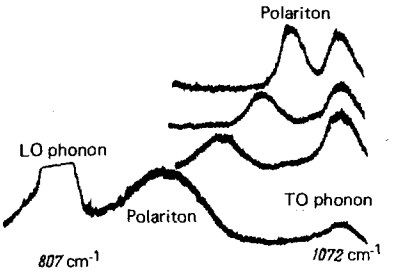

FIG. 25. Spectra of the light scattered by polaritons in a quartz crystal obtained at various scattering angles.[11]

$$w=\frac{2\pi}{\hbar}|\hat{\mathcal{H}}'^{(3)}_{fi}|^2\delta(\varepsilon_f-\varepsilon_i).$$

We shall now introduce the light flux $P(\Omega)$ scattered into a unit solid angle near the direction $\Omega=\mathbf{k}_s/k_s$ and we shall describe this light flux by $P(\Omega)=\hbar\omega_s w(\Omega)N_l=\hbar\omega_s w(\Omega)VI_l/v_l\hbar\omega_l$, where N_l is the number of the exciting radiation photons in a region of volume V, $I_l=(N_l/V)v_l\hbar\omega_l$ is the intensity of the exciting radiation (i.e., the flux per unit surface area), and v_l is the group velocity. The results of a calculation carried out in the approximation of a plane linearly polarized monochromatic pump wave, carried out subject to the conservation laws (3.1), give[48]

$$P(\Omega)=\frac{2\pi\hbar VI_l}{c^5 n_l\gamma_l}\frac{\omega_s^4\omega v_s v n_s|\chi|^2}{n\gamma\gamma_s|v_s\gamma_s-v\cos\psi|};\qquad(5.1)$$

here, v is the group velocity; γ is the cosine of the angle between the group and phase velocities; $\cos\psi=(k_l\cos\varphi-k_s)/k$; φ is the scattering angle; ψ is the angle between $\mathbf{k}$ and $\mathbf{k}_s$; $\chi=e_i^s e_j e_k^l\chi_{ijk}(-\omega,\omega_l)$; $\mathbf{e}$ are the unit polarization vectors of the electric fields involved; χ_{ijk} is the nonlinear susceptibility tensor,[108-112] which governs the generation of the sum frequency $\omega_s=-\omega+\omega_l$ and which occurs in the relationship $P_i^s=\chi_{ijk}E_j^* E_k^l$; $\mathbf{P}^s$, $\mathbf{E}$, and $\mathbf{E}^l$ are the complex amplitudes of the corresponding waves, for example,

$$\mathbf{F}^l(r,\ t)=\mathbf{E}^l\exp[i(k_l r-\omega_l t)]+\text{ c.c.},\ \mathbf{E}^l=\mathbf{e}^l E^l.$$

When polaritons travel along the optical axis of a cubic or a uniaxial crystal, the expression for $P(\mathbf{E})$ should be summed over the two polariton polarizations. The following relationships are used in the derivation of Eq. (5.1):

$$\delta[\omega_s(\mathbf{k}_s)+\omega(\mathbf{k}_l-\mathbf{k}_s)-\omega_l]=\sum_i\left|\left(\frac{\partial[\omega_s(\mathbf{k}_s)+\omega(\mathbf{k}_l-\mathbf{k}_s)]}{\partial k_s}\right)_{k_s=k_s^i}\right|^{-1}\delta(k_s-k_s^i)$$

and

$$\frac{\partial[\omega_s(\mathbf{k}_s)+\omega(\mathbf{k}_l-\mathbf{k}_s)]}{\partial k_s}=v_s\gamma_s-v\cos\psi=\Omega(\mathbf{v}_s-\mathbf{v}),$$

where the index i labels the various roots of the equations $\omega_s(\mathbf{k}_s)+\omega(\mathbf{k}_l-\mathbf{k}_s)-\omega_l=0$ for k_s and the derivative with respect to k_s is calculated for a fixed value of Ω.

a) Integrated scattered-light intensity

The relationship (5.1) is a general formula describing parametric scattering. The integrated intensity of light which is Raman-scattered by polaritons can be found if we start with the familiar quantum-mechanical expression for the nonlinear susceptibility tensor.[110,111] Since

the Raman scattering process usually satisfies the condition $\omega_{l,s} \gg \omega$ and if additionally the frequencies $\omega_{l,s}$ are in the transparency range of a given crystal, the tensor χ_{ijk} can be divided into two parts: χ^E_{ijk} which shows no resonance when ω is varied and which is governed by the contribution of levels distant from the polariton frequency ω and the resonance part containing energy factors $\hbar(\omega_f \pm \omega)$. The part χ^E_{ijk} usually corresponds to the pure electronic contribution to $\chi_{ijk}(-\omega, \omega_l)$ and the resonance part to a mixed electronic–ionic contribution.

Using the definition of the tensor of the "conventional" Raman scattering of light per unit cell,

$$\alpha_{ij}(\omega_l, \omega_s) = \frac{1}{2\hbar} \sum_n \left(\frac{d^j_{0n} d^i_{nf}}{\omega_n - \omega_l} + \frac{d^i_{0n} d^j_{nf}}{\omega_n + \omega_s} \right), \tag{5.2}$$

where d_{mn} is the matrix element of the dipole moment operator of a unit cell, we can express the nonlinear susceptibility tensor $\chi_{ijk}(-\omega, \omega_l)$ in the form

$$\chi_{ijk}(-\omega, \omega_l) = \chi^E_{ijk} + \frac{2\sqrt{N}}{\hbar} \sum_f^M \frac{\omega_f P^j_f \alpha_{ik}}{\omega_f^2 - \omega^2} = \chi^E_{ijk} + \frac{2\sqrt{N}}{\hbar} \sum_f^M \frac{\omega_f P_f \alpha^j_{ik}}{\omega_f^2 - \omega^2}; \tag{5.3}$$

here, $\mathbf{P}_f = \mathbf{P}_{0f} = \mathbf{d}_{0f}/V_0$; $\mathbf{P}_f = \mathbf{e}_f P_f$ $(e_f = 1)$; M is the number of the dipole-active vibrations; V_0 is the volume of a unit cell; $\alpha^j_{ik} = e_{fj}\alpha_{ik}$; N is the total numberof unit cells in the scattering zone. The convolution of the nonlinear susceptibility tensor χ_{ijk} with the corresponding polarization unit vectors is

$$\chi = \chi_{ijk}(-\omega, \omega_l) e^s_i e_j e^l_k = \frac{2\sqrt{N}}{\hbar} \sum_f \left[1 + A_f \left(1 - \frac{\omega^2}{\omega_f^2} \right) \right] \frac{\omega_f P_f}{\omega_f^2 - \omega^2} \alpha^j_{ik} e^s_i e_j e^l_k, \tag{5.4}$$

where

$$A_f = \frac{\hbar\omega_f}{2P_f\sqrt{N}} \frac{\chi^E_{ijk} e^s_i e_j e^l_k}{\alpha^j_{ik} e^s_i e_j e^l_k}. \tag{5.5}$$

Substituting Eq. (5.4) into Eq. (5.1), using the expression for the flux of light Raman-scattered by transverse optical phonons

$$P_f(\Omega) = N \left(\frac{\omega_s}{c} \right)^4 \frac{n_s}{\gamma_s^2} \frac{I_l}{n_l \gamma_l} (\alpha^j_{ik} e^s_i e_j e^l_k)^2, \tag{5.6}$$

and bearing in mind also that $n = \sqrt{\varepsilon(\omega)}$, where $\varepsilon(\omega)$ is governed by the relevant expressions in Sec. 2 (the oscillator strength S_f can be described, in terms of the parameters employed in that section, by the expression $S_f = 8\pi V |P_f|^2/\hbar\omega_f$), we obtain for $P(\Omega)$ the equation[96,97]

$$P(\Omega) = \left| \sum_f \sqrt{P_f(\Omega) \Pi_f \left[1 + A_f \left(1 - \frac{\omega^2}{\omega_f^2} \right) \right]^2} \operatorname{sign} Q_f \right|^2; \tag{5.7}$$

here,

$$Q_f = \left(A_f + \frac{\omega_f^2}{\omega_f^2 - \omega^2} \right) \alpha^j_{ik} e^s_i e_j e^l_k, \tag{5.8}$$

$$\Pi_f = \frac{8\pi V \omega_f^3 \omega |P_f|^2}{c\hbar n (\omega_f^2 - \omega^2)^2 \gamma |v^{-1} - (v_s\gamma_s)^{-1} \cos\psi|} = \frac{\omega_f \partial n/\partial\omega}{|n + \omega(\partial n/\partial\omega) - (c/v_s\gamma_s\gamma)\cos\psi|}. \tag{5.9}$$

We shall consider the physical meaning of the quantities occurring in Eq. (5.7). We shall do this for the case of a crystal with one phonon energy band. In this case the expression (5.7) becomes

$$P(\Omega) = P_f(\Omega) \Pi_f \left[1 + A_f \left(1 - \frac{\omega^2}{\omega_f^2} \right) \right]^2. \tag{5.10}$$

The quantity Π_f is known as the polariton factor[96,97] and it describes the influence on the scattering intensity of the mixing of lattice vibrations with a transverse electromagnetic field. It follows from Eq. (5.9) that the problem of finding Π_f effectively reduces to the determination of the dependences $\omega(\varphi)$ and $\psi(\varphi)$ (see Sec. 3). The polariton factor is important in the range where a phonon is converted into a polariton. In fact, for $\omega - \omega_f$ and $\Pi_f \to 1$, Eq. (5.10) reduces to Eq. (5.6). The polariton factor, i.e., the influence of the polariton dispersion on the density of the final states resulting from the decay of an exciting radiation photon into a Stokes quantum and a polariton, is ignored in some of the early theoretical treatments;[101-104] this factor may differ considerably from unity[96-98] and it increases as the separation between ω and the phonon frequency ω_f increases. In other words, the integrated intensity of the scattered radiation depends on the angle between the tangents to the $q(\omega)$ and $k(\omega)$ curves (see Sec. 3). In fact, the smaller is the angle between the tangents, the wider is the scattering spectrum and, consequently, the higher is the integrated scattered-light intensity. In the range of large scattering angles this angle is of the order of 90° and the scattering line width is governed only by the phonon line width.

It is clear from Eq. (5.5) that the quantity A_f is the ratio of the electronic and electron–ionic contributions to the nonlinear susceptibility and it is called[98] the electron–deformation parameter of the crystal for the vibration ω_f. Thus, the factor $[1 + A_f(1 - (\omega^2/\omega_f^2))]$ describes the relative contribution of the electron processes in the lattice polarization to the intensity of the Raman scattering of light by polaritons of frequency ω. When the frequency ω approaches ω_f, the relative contribution of the electron processes decreases and

$$\left[1 + A_f \left(1 - \frac{\omega^2}{\omega_f^2} \right) \right] \to 1,$$

i.e., the scattering intensity is then governed only by the tensor α^j_{ik}.

In the general case of an arbitrary number of the phonon energy bands the various vibrational transitions interfere with one another and the result depends on the relative signs of the contributions of these transitions, which are governed by the signs of the quantities Q_f in Eq. (5.7).

Equation (5.7) can also be used to obtain directly the expression for the light flux scattered by longitudinal optical phonons $P_{fL}(\Omega)$ if e is replaced by the polarization unit vector of an LO phonon, ω is replaced by ω_L, and it is assumed that $n = 0$.

b) Profile of Raman lines for scattering by polaritons

It is convenient to study the scattering line profile within the framework of the fluctuation–dissipation method[97] in which the appearance of the scattered radiation is regarded as the result of mixing of the exciting radiation with an equilibrium electromagnetic noise in the investigated medium. The results of a calculation for the isotropic case give the following expression for the spectral density of the scattered light flux $P(\Omega, \omega)$:

$$P(\Omega)=\int_0^\infty P(\Omega,\ \omega)\,d\omega,$$
$$P(\Omega,\ \omega)=\frac{P(\Omega)}{\pi}\frac{\varepsilon''(\omega)}{[(|\mathbf{k}_l-\mathbf{k}_s|\,c/\omega)-\varepsilon(\omega)]^2+[\varepsilon''(\omega)]^2},\qquad (5.11)$$

where $\varepsilon(\omega)$ is given by the appropriate relationship in Sec. 2 and $\varepsilon''(\omega)$ is the imaginary part of the complex permittivity at the polariton frequency. The expression (5.11) is valid if the polariton line is separated from the phonon line by an interval $\omega_f-\omega$ considerably greater than the phonon line half-width. In this region we can regard χ as real and ignore the dispersion of $P(\Omega)$ within the polariton line profile and take $P(\Omega)$ at the line center. In view of the smallness of $\varepsilon''(\omega)$ in this range, we can represent $P(\Omega,\omega)$ approximately in the form

$$P(\Omega,\ \omega)=\frac{P(\Omega)}{\pi}\frac{\gamma/2}{(\omega_l-\omega_s-\omega)^2+(\gamma/2)^2},\qquad \gamma=\frac{\omega\varepsilon''(\omega)}{cn[v_s^{-1}\cos\psi-v^{-1}]}.\qquad (5.12)$$

It follows that the scattered-line profile is Lorentzian, its half-width is γ, and the scattered light flux at the maximum is $2P(\Omega)(\pi\gamma)^{-1}$. The presence of the factor $(v_s^{-1}\cos\psi-v^{-1}$ in Eq. (5.12) reflects the fact that the line width of the scattered radiation depends not only on the polariton attenuation but, as mentioned above, on the changes in the conservation laws during scattering. It should be noted that the representation (5.12) ceases to be valid in the presence of group phase matching when $v_s^{-1}\cos\psi-v^{-1}=(v_sv)^{-1}\mathbf{\Omega}(\mathbf{v}-\mathbf{v}_s)=0$. This is equivalent to the condition $d\varphi/d\omega=0$, which is satisfied when then graph of the function $q(\omega)$ is tangent to the function $k(\omega)$. Then, instead of Eq. (5.12) we have to use the more general expression (5.11). The integrated scattering intensity then rises steeply (because of strong broadening of the scattered line) but remains finite. However, according to Eq. (5.9), the polariton factor becomes infinite. We can avoid this by taking greater care in making the transition from the scattering line profile to the integrated intensity.[98]

We shall conclude this section by giving the appropriate expressions for the scattering of light by longitudinal optical phonons obtained in the approximation when ω_L is separated from ω_f by a considerable distance compared with the phonon attenuation constant:

$$P_{fL}(\Omega)=\int_0^\infty P_{fL}(\Omega,\ \omega)\,d\omega,$$
$$P_{fL}(\Omega,\ \omega)=\frac{P_{fL}(\Omega)}{\pi}\frac{\gamma_{fL}/2}{(\omega_l-\omega_s-\omega)^2+(\gamma_{fL}/2)^2},$$
$$\omega_l-\omega_s=\omega_{fL},$$
$$\gamma_{fL}=2\varepsilon''(\omega_{fL})\left(\frac{\partial\varepsilon(\omega)}{\partial\omega}\right)^{-1}_{\omega=\omega_{fL}}.$$

In the case of an isolated phonon energy band, we have $\gamma_{fL}=\gamma_f$.

In the above treatment we have always ignored thermal fluctuations and considered only those of quantum origin. Allowance for thermal fluctuations in the Stokes scattering case gives rise, in the expressions for $P(\Omega,\omega)$ and $P_{fL}(\Omega,\omega)$ of the factor $\coth[\hbar(\omega_l-\omega_s)/2k_0T]$, where k_0 is the Boltzmann constant.

6) RELATIONSHIP OF RAMAN SCATTERING BY POLARITONS TO RAMAN SCATTERING BY OPTICAL PHONONS, SECOND HARMONIC GENERATION, AND LINEAR ELECTROOPTIC EFFECT

The nonlinear susceptibility tensor describing the Raman scattering of light by polaritons consists—according to Eq. (5.3)—of a resonance and a nonresonance part. If the polariton frequency ω is sufficiently far from the lattice resonance frequencies $\omega_f(\omega\gg\omega_f)$, the scattering process can be described satisfactorily by the nonresonance part χ^E_{ijk} of the nonlinear susceptibility tensor. In the limit $\omega\to\omega_s$ the tensor $\chi^E_{ijk}(-\omega,\omega_l)$ can be identified with the tensor $\chi_{ijk}(\omega,\omega)\equiv\chi^{2\omega}_{ijk}$ responsible for second harmonic generation.[108-112] In fact, if the permutation relationships for the frequencies and indices i, j, and k are taken into account, we obtain

$$e^s_ie^l_je^l_k\chi^E_{ijk}(-\omega,\ \omega_l)=e^l_ke^s_ie^s_j\chi_{kij}(\omega,\ \omega_s)=e^l_ke^s_ie^s_j\chi^{2\omega}_{kij}.\qquad (6.1)$$

The tensor $\chi^{2\omega}_{kij}$ is symmetric with respect to the last two indices.

Moreover, in the limit $\omega\to0$ the tensor $\chi_{ijk}(0,\omega_l)$ describes not only the Raman scattering of light by low-frequency polaritons but also the linear electrooptic effect. The tensor $r_{ijk}(0,\omega_l)$ is related to the electrooptic tensor $\chi_{ijk}(0,\omega_l)$ by:[112]

$$\chi_{ijk}(0,\ \omega_l)=-\frac{\varepsilon_i(\omega_l)\,\varepsilon_k(\omega_l)}{4\pi}r_{ikj}(0,\ \omega_l).\qquad (6.2)$$

The tensor r_{ikj} is symmetric with respect to the first two indices and its value may be found by measurements on clamped crystals, i.e., by measurements carried out at frequencies of external electric fields exceeding the fundamental frequencies of piezoelectric resonances in a crystal. This requirement is usually satisfied by frequencies $\gtrsim1$ MHz. Equation (5.3), together with Eqs. (6.1) and (6.2), gives

$$-\frac{\varepsilon_i(\omega_l)\,\varepsilon_k(\omega_l)}{4\pi}r_{ikj}=\chi^{2\omega}_{kij}+\frac{2\sqrt{N}}{\hbar}\sum_f^M\frac{P_f}{\omega_f}\alpha^j_{ik}.\qquad (6.3)$$

Using the definition of the electron–deformation potential, we can rewrite Eq. (6.3) also in the form

$$-\frac{\varepsilon_i(\omega_l)\,\varepsilon_k(\omega_l)}{4\pi}r_{ikj}e^s_ie^l_ke_j=\sum_f^M\frac{2\sqrt{N}}{\hbar}(1+A_f)\frac{P_f}{\omega_f}\alpha^j_{ik}e^s_ie^l_ke_j=\left(1+\frac{1}{M}\sum_f^M\frac{1}{A_f}\right)\chi^{2\omega}_{kij}e^l_ke^s_ie_j.\qquad (6.4)$$

For simplicity, we shall consider diatomic crystals. The results of Sec. 5 can be used to obtain an expression for the ratio of the intensities of light scattered by longitudinal and transverse optical phonons. If the scattering geometry is such that the corresponding convolutions in the expressions for $P_f(\Omega)$ and $P_{fL}(\Omega)$ are identical, then $A_{fL}=A_f$ and

$$\frac{P_{fl}(\Omega)}{P_f(\Omega)}=\left(\frac{\omega_l-\omega_{fL}}{\omega_l-\omega_f}\right)^4\left[1+A_f\left(1-\frac{\omega^2_{fL}}{\omega^2_f}\right)\right]^2\frac{\omega_f}{\omega_{fL}}\frac{\tilde n_{fL}+1}{\tilde n_f+1},\qquad (6.5)$$

where $\tilde n_{fL}=[\exp(\hbar\omega_{fL}/k_0T)-1]^{-1}$ and $\tilde n_f=[\exp(\hbar\omega_f/k_0T)-1]^{-1}$. These expressions establish the relationship between the tensors describing optical harmonic generation, linear electrooptic effect, and Raman scattering of light by optical phonons. Combining these relationships, we can, for example, express the nonlinear coefficients r_{ikj} and $\chi^{2\omega}_{kij}$ in terms of quantities which can

be deduced from measurements of the Raman scattering of light by optical phonons:

$$A_f = \left(1 \pm \sqrt{\frac{P_{fL}(\Omega)\,\omega_{fL}}{P_f(\Omega)\,\omega_f}}\right) \frac{\omega_l - \omega_f}{\omega_l - \omega_{fL}} \sqrt{\frac{\bar{n}_f + 1}{\bar{n}_{fL} + 1}} \frac{\omega_f^2}{\omega_{fL}^2 - \omega_f^2}, \quad (6.6)$$

$$\chi_{kij}^{2\omega} = -\frac{\varepsilon_i(\omega_l)\,\varepsilon_k(\omega_l)}{4\pi} r_{ikj} (1 + A_f^{-1})^{-1}, \quad (6.7)$$

$$r_{ikj} = -\frac{4\pi(1 + A_f)}{\varepsilon_i(\omega_l)\,\varepsilon_k(\omega_l)} \sqrt{\frac{S_f}{2\pi V_0 \hbar \omega_f}}\, \alpha_{ik}^j. \quad (6.8)$$

It should be noted that measurements of the ratio of the intensities of light scattered by longitudinal and transverse optical phonons give a unique value of A_f. The choice of the sign of the root can be settled unambiguously by, for example, comparing the values of $\chi_{kij}^{2\omega}$ and r_{ikj} obtained from Eqs. (6.7) and (6.8) with the results of direct measurements of these quantities.[121]

An interesting feature of Eq. (5.4) is that the nonlinear susceptibility and, consequently, the scattering intensity vanishes at the polariton frequency $\omega = \omega_{\min}$, given by

$$\omega_{\min}^2 = (1 + A_f^{-1})\,\omega_f^2. \quad (6.9)$$

This vanishing of the intensity of light scattered by polaritons is a consequence of the compensation of the electronic and lattice contributions to the nonlinear susceptibility. This effect was first demonstrated experimentally by Faust and Henry[123] in investigations of optical mixing processes in GaP crystal. Somewhat later the compensation effect was also discovered in an investigation of the Raman scattering of light by polaritons of the upper dispersion branch of a polyatomic lithium niobate crystal.[14] This work has played an important role in the understanding of the influence of absorption of the idler wave on the intensity of the parametric scattering of light.[126] It should also be noted that in the case of a diatomic crystal the value of the frequency $\omega_{\min}$ at which the intensity of the scattered light vanishes can be used to find directly both the magnitude and sign of the electron–deformation parameter A_f.

The magnitudes and signs of the electron–deformation parameters A_f of some diatomic crystals have now been deduced from the experimental data on the Raman scattering of light. These values of A_f and some other parameters of the investigated crystals are listed in Tables I and II. It is worth noting that $4d_{14} = \chi_{123}^{2\omega}$[121]; moreover, in some cases the parameter A_f is replaced by

TABLE I. Parameters of diatomic cubic crystals of point symmetry group $\bar{4}3m$ obtained from Raman scattering experiments.

Crystal	ν_{TO}, cm^{-1}	ν_{LO}, cm^{-1}	r_{41}, 10^{-12} m/V	d_{14}, 10^{-12} m/V	A_f	$\frac{P_{fL}}{P_f}$	λ_l, nm	Reference
CuCl *)	147	211	−0.4	6.8	−1.3		514.5	120
	159	211	0.4	−4.9	−0.8		514.5	120
CuBr *)	134	167	−0.6	−15.8	−0.8		514.5	120
CuI *)	131	149	±5.3	19.4	0.9		514.5	120
GaAs	269	292	1.5	140	−1.7		1060	121
	269	292	1.5	100	−2.2		1060	122
GaP	365	403			−1.9	1.73	632.8	123
ZnSe	204	251			−4.8	8.5	632.8	104
					−4		568.2	41
					−8		488	41
						100	632.8	104
ZnS	274	349			−5.6 or 8.9	15	514.5	124

*)The measurements were carried out with the samples kept at 60 °K.

TABLE II. Parameters of diatomic uniaxial crystals of point symmetry group $6mm$ obtained from Raman scattering experiments.

Crystal	Vibration symmetry	ν_{TO}, cm^{-1}	ν_{LO}, cm^{-1}	A_f	$\frac{P_{fL}}{P_f}$	λ_l, nm	Reference
ZnO	$A_1(zz)$	381	574	1.7	0.83	632.8	104
	E_1	407	583	1.4	0.18	632.8	104
	E_1			1.8	0.5	514.5	126
CdS	$A_1(xx)$	228	305	2.0		514.5	51
	$A_1(zz)$			2.0		514.5	51
	E_1	235	305	4.3		514.5	51

other parameters related in the following way to A_f:

$$A_f = \frac{1}{C}\ ^{123}, \quad A_f = \gamma\ ^{51}, \quad A_f = \frac{4\pi N}{\varepsilon_0} \frac{e_f^* b}{a} \frac{\omega_f^2}{\omega_{fL}^2 - \omega_f^2}\ ^{104}.$$

The situation becomes more complicated in the case of polyatomic crystals. We then have to use Eqs. (6.3) and (6.4). Since the constants A_f can be determined for various phonon branches from the absolute intensities of the light scattered by transverse optical phonons and from the measured values of $\chi_{ijk}^{2\omega}$, the main difficulty is to select the sign of A_f. One of the methods of determining the sign of A_f is to select such a combination of signs of A_f so as to obtain from Eq. (6.4) the best approximation to the quantity r_{ijk} deduced from independent measurements. This gives 2^M possible combinations and, therefore, in the case of a large number (M) of phonon energy bands the required combination cannot always be found unambiguously. Experimental determination of the existence of the compensation effect in the scattering of light by polaritons of the upper dispersion branch provides useful complementary evidence which can be used to select correctly the combination of signs. A rough estimate of the position of the minimum ω_{min} of the intensity of the scattered light can be obtained by assuming that $\omega_{min} \gg \omega_f$:

$$\omega_{\min}^2 = \frac{1}{M} \sum_f^M \frac{\omega_f^2}{A_f}. \quad (6.10)$$

Using the results for the Raman scattering of light by optical phonons, second harmonic generation, and linear electrooptic effect in lithium niobate, as well as the fact that the compensation point occurs at $\nu_{\min} \approx 1500$ cm^{-1}, Obukhovskii *et al.*[99] were able to select a combination of signs and magnitudes of A_f for this crystal. The results were used in Ref. 99 to calculate the frequency dependences of the intensity of light scattered by polaritons in various scattering geometries.[8)] However, it should be noted that the correctness of the selection of the parameters used can be checked by direct measurements of these dependences. Unfortunately, practically no investigations of this kind have been carried out for polyatomic crystals.

7. SOME CHARACTERISTICS OF POLARITON SPECTRA

In this section we shall consider briefly some features of polariton spectra which cannot be described in

8)The recent identifications of the symmetry of the optical vibrations in an $LiNbO_3$ crystal[132] would require some corrections of the above calculations.

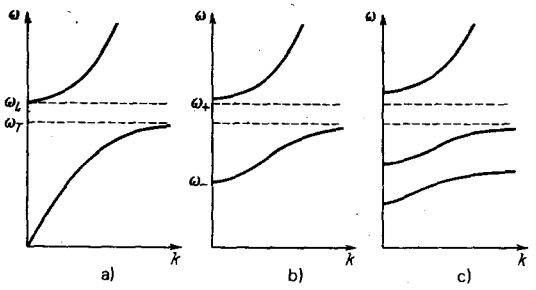

FIG. 26. Polariton dispersion in a diatomic cubic crystal, (a) in the absence of free carriers, (b) in the presence of free carriers, and (c) in the presence of free carriers and a transverse magnetic field B (k⊥ B).

terms of the above model. These features are manifest, for example, when free carriers, localized modes, bands of two-particle states, etc. are present in a crystal.

a) Influence of free carriers

The nature of photon propagation in a medium changes fundamentally in the presence of free carriers (electron or hole plasma). For example, the propagation of photons is impossible at frequencies below the plasma value since the permittivity is then purely imaginary. However, at higher frequencies we can expect propagation of mixed photon–phonon–plasmon excitations or of phonon–plasmon polaritons (plasmoritons). The dispersion of phonon–plasmon polaritons in a cubic diatomic crystal[9)] is described by:[127]

$$\frac{k^2c^2}{\omega^2}=\varepsilon_\infty\left(1-\frac{\omega_p^2}{\omega^2}\right)+\frac{(\varepsilon_0-\varepsilon_\infty)}{\omega_T^2-\omega^2}\omega_T^2, \qquad (7.1)$$

where $\omega_p=\sqrt{4\pi Ne^2/m^*\varepsilon_\infty}$ is the plasma frequency; N, e, and m^* are the density, charge, and effective mass of free carriers, respectively. The influence of free carriers on the polariton dispersion is illustrated in Figs. 26a and 26b. The frequencies ω_+ and ω_- are found from Eq. (7.1) using the expression

$$\omega_\pm^2=\frac{1}{2}(\omega_L^2+\omega_p^2)\pm\frac{1}{2}\sqrt{(\omega_L^2+\omega_p^2)^2-4\omega_T^2\omega_p^2}.$$

It is worth noting (see Fig. 26b) that photon propagation is impossible at frequencies below ω_-. However, application of an external magnetic field B induces modes capable of propagation at frequencies below ω_-. Then, mixed photon–phonon–plasmon–cyclotron excitations or photon–magnetoplasma polaritons (magnetoplasmoritons) may appear in a crystal. In this case the polariton dispersion (in the k ⊥ B case) has the form shown in Fig. 26c. The theory of the Raman scattering of light by polaritons in the presence of free carriers in a crystal is discussed by Wolff and Blum.[129]

The influence of free carriers on the polariton dispersion has been observed successfully by experimental methods. Investigations have been carried out on diatomic cubic semiconductor crystals of GaAs (Ref. 4) and CdS (Ref. 50) by the Raman scattering of light at low angles. Measurements of the polariton dispersion in these crystals carried out for a range of carrier densities $N=6.7\times10^{16}$, 1.4×10^{17}, and 2.9×10^{17} cm^{-3} for a GaAs crystal (Ref. 4) and $N=10^{15}$, 4×10^{18}, and 2×10^{-19} cm^{-3} for a CdS crystal (Ref. 50) agree well with the data calculated on the basis of Eq. (7.1). Moreover, it is reported in Ref. 4 that the polariton dispersion changes on application of an external transverse (B ⊥ k) magnetic field ($B=100$ kOe for $N=2.9\times10^{17}$ cm^{-3}). This is evidence of the presence of phonon–magnetoplasma polaritons (magnetoplasmoritons). However, it should be pointed out that Patel and Slusher[4] failed to detect magnetoplasmoritons corresponding to the lowest dispersion branch in Fig. 26c and this was probably due to the fairly small cross section for the scattering by excitations in this branch.[129]

b) Influence of localized modes

We have discussed so far the polariton spectra of ideal crystals. However, the presence of defects in a crystal may give rise to additional optical modes and to their interaction with polaritons. We shall consider a crystal with the simplest defect in the form of an atom whose mass differs from the masses of the lattice atoms. Such defects are frequently encountered in crystals prepared from a material with a natural mixture of isotopes. At low defect (isotope) concentrations the vibrations of impurity atoms can be regarded as localized. In the case of rigorously localized modes the amplitudes decrease exponentially with distance from the impurity position.

If the impurity modes are dipole-active, they can interact with electromagnetic waves in the range of low values of k and this produces localized polariton modes. Consequently, in the vicinity of localized modes there may be considerable deviation of the polariton dispersion from the results calculated using the parameters of an ideal crystal.

The polariton dispersion of diatomic cubic crystals containing localized modes has the form[130]

$$\frac{k^2c^2}{\omega^2}=\varepsilon_\infty+\frac{S\omega_T^2}{\omega_T^2-\omega^2}+\frac{S_g\omega_{Tg}^2\xi(\omega_{Tg})}{\omega_{Tg}^2-\omega^2}, \qquad (7.2)$$

where ω_{Tg} is the frequency of a transverse localized mode;

$$\xi(\omega_{Tg})=|\chi g|^2M'-\left(1-\frac{M'_-}{M_-}\right)^2\times\left(1-\frac{\omega_T^2}{\omega_{Tg}^2}\right),$$

M_- and M'_- are the masses of the negative lattice and impurity ions. The first two terms on the right-hand side of Eq. (7.2) describe polariton dispersion in an ideal crystal and the third term is due to a localized mode.

The first successful observation of localized polariton modes was reported by Nitsch and Claus[131] who investigated the Raman scattering of light at small angles in a $K_3Cu(CN)_4$ crystal. They observed four localized polariton modes of vibrations of the C≡N bond, due to the natural abundances of the C^{13} and N^{15} isotopes in the original substance; the abundances of these isotopes were 1.12 and 0.36%, respectively.

Figure 27 shows, by way of example, the Raman scattering of light at small angles in a $K_3Cu(CN)_4$ crystal,

[9)] The dispersion of phonon–plasmon polaritons in uniaxial crystals is discussed in Ref. 128.

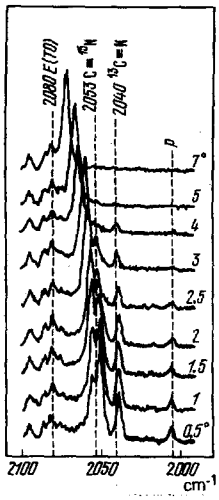

FIG. 27. Spectra of the Raman scattering of light by E polaritons in a $K_3Cu(CN)_4$ crystal obtained at various scattering angles. Here, p is the plasma line of the gas discharge used in the laser.

illustrating the interaction between the E polaritons and two localized modes.[49,131] The points in Fig. 28 are the polariton dispersion curves deduced from the spectra in Fig. 27. The dashed curve in Fig. 28 represents calculations carried out ignoring localized modes, whereas the continuous curves are the calculations based on a formula of the (7.2) type but generalized to the case of a polyatomic crystal[136] using the values of the parameter $M_-'|\chi_\varepsilon|^2 = 0.3$, 0.6, and 1.0.

Thus, the polariton dispersion is modified greatly by the presence of impurities in a crystal. The dispersion can then be described in terms of the theory developed by Ohtaka[130] and Nitsch.[136] It should be mentioned that a satisfactory description of the experimental results was not obtained in Refs. 49 and 131 when an earlier theory[137] was used.

An interesting feature of the spectra shown in Fig. 27 is the transfer of excitation from polaritons to localized modes in the scattering spectra as the polariton frequency approaches the localized mode frequency. The increase in the intensity of the light scattered by localized modes because of the interaction with polaritons may play an important role in the detection of localized modes because the intensity of light scattered by these excitations is usually quite low.

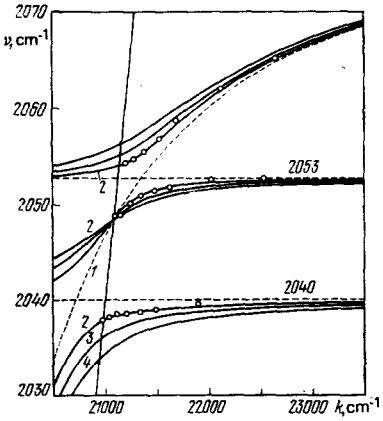

FIG. 28. Dispersion of the E polaritons in the region of interaction with localized modes. The circles are the experimental data; the dashed curve 1 is calculated ignoring localized modes and the continuous curves are computed allowing for localized modes and using the following values of the parameter $M_-'|\chi_\varepsilon|^2$: 2) 0.3; 3) 0.6; 4) 1.0.

It should be mentioned that the interaction of polaritons with localized modes was observed also in an $NaClO_3$ crystal.[138] The localized modes in this crystal are due to the presence of the ^{35}Cl and ^{37}Cl isotopes.

c) Interaction of polaritons with energy bands of two-particle states

Near overtones and combination frequencies of vibrations of a crystal lattice the Raman spectra usually have not narrow lines, as is the case in isolated molecules, but wide bands, corresponding to two-particle bands of states as a result of phonon dispersion in the Brillouin zone. If the two-particle excitations are dipole-active, then in the region of "intersection" of a polariton branch with a band of two-particle states there is an interaction between these excitations and this alters the spectra considerably. The resultant phenomenon is known as a polariton Fermi resonance. The theory of this phenomenon is given fully in Ref. 140 and, therefore, we shall mention here only some of the conclusions of this theory and then concentrate on some of the experimental data.

Since the Raman scattering of light by polaritons is usually stronger than the scattering by two-particle excitations, it follows that an intersection of a polariton branch with a band of two-particle states always results in transfer of the Raman-scattered light from polaritons to two-particle states. Within a two-particle band there may be nonmonotonic changes in the polariton frequency, depending on the wave vector k, and these may be accompanied by broadening of the Raman line. This broadening is due to the possibility of decay of a polariton into two free phonons.

The first experimental observations of a polariton Fermi resonance were reported in Ref. 47 but subsequent detailed studies have shown that the observed effect can be due to interaction of polaritons with localized modes.[131] The results of Ref. 54 cannot be interpreted unambiguously because of the presence, in the investigated part of the spectrum, of a weak first-order Raman line of symmetry other than the polariton symmetry. Therefore, it follows from the scattering geometry used in Ref. 54 that the observed features of the scattering spectra can be explained also by an anti-intersection of polariton branches[74] (see also Sec. 2.c). The most convincing observations of a polariton Fermi resonance were made on $LiNbO_3$ (Refs. 16 and 20) and $LiIO_3$ (Refs. 35–37) crystals for which a detailed interpretation of the first-order phonon spectrum was provided. An energy gap in the polariton scattering spectrum was observed in Ref. 20 under Fermi resonance conditions and this was attributed[140] to the existence of coupled (biphonon) states of two phonons.[10)] However,

[10)] A theoretical analysis of the formation of biphonons can be found also in Ref. 141.

experiments carried out on an NH_4Cl crystal (Ref. 7) showed that the appearance of an energy gap in the polariton branch under polariton Fermi resonance conditions need not be necessarily due to the existence of biphonons. Moreover, the polariton dispersion in the region of the second-order phonon spectrum of an $LiNbO_3$ crystal cannot be described by introducing an oscillator strength and a limiting frequency,[16] which would have been possible if biphonons were present.[140] In the case of an $LiIO_3$ crystal there are several "discontinuities" of the polariton branch corresponding to polariton Fermi resonances in the range ~1500–1650 cm^{-1} (Refs. 35–37). Some singularities of the Raman scattering by polaritons have been observed also in the spectra of more complex crystals[53,55-57,80,81] and these cannot be attributed to the first-order phonon spectra. Nevertheless, some features of these spectra can definitely be attributed to polariton Fermi resonances.

Interesting results on the general properties of polariton Fermi resonances are obtained also by investigating the behavior of polariton scattering spectra within a band of two-particle states. From this point of view, the NH_4Cl crystal is one of the most interesting objects. A detailed attribution of the optical vibrations to specific symmetries has been made on the basis of the first- and second-order Raman spectra of this crystal.[133,134] In particular, a wide (~110 cm^{-1}) isolated band of two-particle states $2\nu_4(F_2)$ has been identified.[134] It should be noted that the reported singularities of polariton scattering spectra within a band of two-particle states, observed under polariton Fermi resonance conditions, cannot be attributed to an isolated band. This is due to the fact that the complexity of the first-order phonon spectra of these crystals results in overlap of the higher-order bands in the spectra. Moreover, sometimes two-particle states of crystals appear in the Raman spectra in the form of sufficiently narrow bands, so that it is not possible to determine the singularities of the polariton scattering spectra within a two-particle band.

In view of this, investigations have been made of the Raman scattering of light by polaritons in an NH_4Cl crystal in the region of a band of two-particle states $2\nu_4$. Figure 29 shows a frequency-angular scattering spectrum of an NH_4Cl crystal in the part of the spectrum corresponding to this band. The spectrogram was obtained with an STÉ-1 spectrograph when the spectral slit width was ~2 cm^{-1} and the temperature of the sample was ~80°K. Exciting argon laser radiation traveled

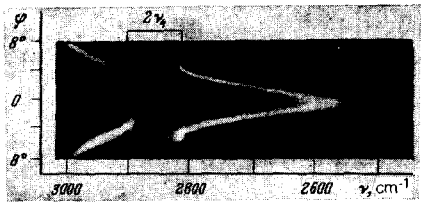

FIG. 29. Fragment of a frequency-angular spectrum of the scattering of light by polaritons in an NH_4Cl crystal ($T = 80$ °K) illustrating the appearance of a Fermi resonance of polaritons with a band of two-particle states $2\nu_4$. Here, φ is the scattering angle inside a crystal; the spectrum was obtained with an STÉ-1 spectrograph.

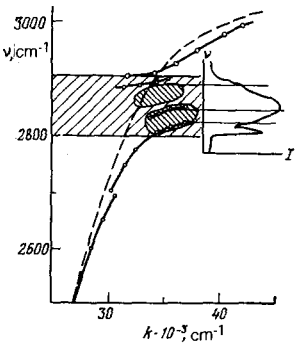

FIG. 30. Dispersion of polaritons in an NH_4Cl crystal in the region of 2500–3000 cm^{-1}. The dashed curve represents calculations carried out ignoring the interaction of polaritons with a band of two-particle states. The continuous curves are deduced from the spectrogram in Fig. 29. The right-hand side shows the Raman spectrum for the scattering at 90°.

along the [110] axis and was polarized along the $[\bar{1}10]$ direction. The scattered radiation traveled in a $(\bar{1}10)$ plane. The frequency-angular scattering spectrum was used to plot the polariton dispersion shown in Fig. 30. The continuous curves represent experimental data corresponding to the intensity maxima in the frequency-angular spectrum of Fig. 29 and the dashed curves represent the polariton dispersion calculated without taking into account the interaction of polaritons with two-particle excitations.

The most interesting and new feature is the observation that within an isolated band of two-particle states there are several polariton regions which appear only in a very limited range of scattering angles (or polariton momenta). Outside these regions the polariton branches inside the two-particle band spread out and merge with the band. The closely shaded regions inside the band in Fig. 30 are those where the intensity exceeds slightly the background scattering inside the two-particle band. The right-hand side of Fig. 30 shows also the spectrum of the conventional Raman scattering of light by two-particle states. It should be noted that there is some correlation between the positions of polariton regions inside the band and "kinks" in the conventional spectrum of the Raman scattering at the two-particle excitations. These kinks are due to density-of-states maxima.

Theoretical investigations[135] of the polariton dispersion within a band of two-particle states have demonstrated the possibility of a strong influence of the critical (Van Hove) points on the polariton dispersion inside this band. The theoretical results[135] are in qualitative agreement with the observed singularities of the polariton dispersion within the two-particle band of the spectra described above. However, according to the theory[135] the polariton dispersion should be continuous inside the two-particle band but the "reverse" dispersion (joining the separate polariton regions) has not been observed experimentally. It is possible that the intensity of the scattering by polaritons in such regions is considerably less than near the critical points. Moreover, the observation of polariton regions near the critical points is, apparently, clear evidence of a reduction in the probability of polariton decay (which is accompanied

by the appearance and the narrowing of polariton regions within the two-particle band) into two phonons. Unfortunately, the available information about the crystal parameters is insufficient for quantitative comparisons of the theory and experiment.

d) Polariton dispersion in gyrotropic crystals

The expression for $\varepsilon(\omega)$ is used above ignoring the spatial dispersion. The influence of the spatial dispersion and, particularly, of the crystal gyrotropy on the polariton dispersion is definitely of interest because such effects may give rise to "new" waves[93] and, consequently, to additional lines in the spectra of the Raman scattering of light by polaritons.

For simplicity, we shall consider a cubic gyrotropic crystal. Then, allowing for the spatial dispersion, the expression

$$\varepsilon(\omega)=\varepsilon_\infty+\frac{S\omega_0^2}{\omega_0^2-\omega^2} \tag{7.3}$$

should be replaced[93] by

$$\varepsilon_{ij}^{-1}(\omega,\ k)=\varepsilon_{ij}^{-1}(\omega)\,\delta_{ij}+i\Delta(\omega)\,e_{ijl}k_l, \tag{7.4}$$

where $\varepsilon(\omega)$ is given by Eq. (7.3) and $\Delta(\omega)$ is some function of ω proportional to the optical rotation. In the absence of absorption the polariton dispersion is then of the form:[93]

$$\left(\frac{1}{\varepsilon(\omega)}-\frac{\omega^2}{c^2k^2}\right)^2=\Delta^2k^2. \tag{7.5}$$

The dependence $\omega(k)$ deduced from Eq. (7.5) is shown schematically in Fig. 31. Optical phonons correspond formally to the limit $c\to\infty$ and, consequently, we have

$$\frac{1}{\varepsilon(\omega)}=\pm|\Delta|k,\qquad \omega_\pm(k)\approx\omega_0\pm\alpha k,\qquad \alpha=\frac{S\omega_0}{2}|\Delta|. \tag{7.6}$$

The branches $\omega_\mp$ are represented by dashed lines in Fig. 31. The splitting of the dispersion branch of the optical phonons due to gyrotropy was first observed for the E mode (128 cm^{-1}) of a quartz crystal.[142] A linear dependence of both frequencies $\omega_\mp$ on k was observed, which was in agreement with Eq. (7.6), and it was found that $\alpha=(0.86\pm0.05)\times10^5$ cm/sec.

An interesting feature of the dispersion curves shown in Fig. 31 is that some frequencies (for example, the frequency identified as ω' in Fig. 31) corresponds to three values of k. This is equivalent to the existence of three solutions (1–3) for $\varepsilon(\omega')$ for a given ω', in contrast to nongyrotropic crystals when only one solution is obtained (compare Figs. 31 and 1). This feature of the polariton spectra of gyrotropic crystals has not yet been observed experimentally.

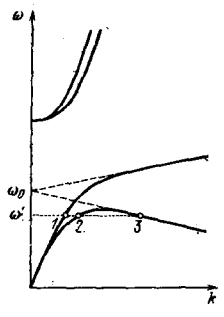

FIG. 31. Polariton dispersion in a cubic diatomic gyrotropic crystal. The dashed lines represent the optical phonon dispersion.

8. COHERENT ANTI-STOKES RAMAN SCATTERING BY POLARITONS

Recent progress in the development of tunable lasers has made it possible to use widely the method of coherent anti-Stokes Raman scattering (CARS) of light[11)] in investigations of various excitations in gases, liquids, and solids. The possibility of using this method in polariton investigations was first demonstrated for a GaP crystal.[143]

The CARS polariton spectroscopy method involves buildup of polariton excitations in the field of two sufficiently strong laser beams of frequencies ω_1 and ω_2, such that the difference between them is equal to the polariton frequency ω_p. If a medium is subjected additionally to a test field of frequency ω (a test wave can be one of the beams participating in coherent buildup of polaritons; for example, let us assume that $\omega_1>\omega_2$ and $\omega=\omega_1$), the test wave is then scattered by polaritons with the same phase throughout the medium and the scattered-light frequency is $\omega_a=\omega_1+\omega_p=2\omega_1-\omega_2$. Since polaritons are characterized by a strong dispersion, the effectiveness of their buildup and, consequently, the intensity of the CARS signal depends not only on the difference between the frequencies of the exciting fields $\omega_1-\omega_2$ but also on the difference between the wave vectors of these fields $\mathbf{k}_1-\mathbf{k}_2$. A study of the dependence of the intensity of the CARS signal on the phase detuning $\Delta\mathbf{k}_p=\mathbf{k}_1-\mathbf{k}_2-\mathbf{k}_p$ is called in Ref. 143 the spectroscopy in k space or k spectroscopy. This dependence is obtained by altering the direction of one of the wave vectors $\mathbf{k}_1$ or $\mathbf{k}_2$ keeping the frequency difference $\omega_1-\omega_2$ fixed. It is shown in Ref. 143 that the polariton attenuation can be deduced from the k spectra. The profiles of the polariton lines in the ω and k spaces can be found also from two-dimensional spectrograms of the Raman scattering of light by polaritons obrained by the photographic method described in Sec. 4. This is done by photometric analysis of a frequency-angular spectrum at a fixed wavelength of the scattered light (k spectra) or at a fixed scattering angle (ω spectra). A modification of the photoelectric method can be used to find not only the ω spectra but also the spectra in k space.[154]

The expression for the intensity of a CARS signal in the polariton case is (see, for example, Ref. 145):

$$I_{as}(\omega_a)\propto I_1^2(\omega_1)I_2(\omega_2)|\chi|^2l^2\left[\frac{\sin(\Delta k\cdot l/2)}{\Delta k\cdot l/2}\right]^2, \tag{8.1}$$

where $I_i(\omega_i)$ is the intensity of the radiation of frequency ω_i; $\Delta\mathbf{k}_a=\mathbf{k}_1+\mathbf{k}_1-\mathbf{k}_2-\mathbf{k}_a$; l is the length of the region of interaction of the light waves; the nonlinear susceptibility tensor χ in the case of strong absorption of a polariton wave can be represented in the form[145]

$$\chi=\chi^{(3)}+\frac{4\pi}{(\Delta k_p c/\omega_1-\omega_2)^2-\varepsilon(\omega_p)}[\chi^{(2)}]^2, \tag{8.2}$$

where $\varepsilon(\omega_p)$ is the complex permittivity which has the

[11)] The term "coherent active combination scattering spectroscopy" is also frequently used in the Soviet literature (see, for example, Ref. 153).

following form for a cubic polyatomic crystal:

$$\varepsilon(\omega_p) = \varepsilon_\infty + \sum \frac{S_j \omega_j^2}{\omega_j^2 - \omega_p^2 - i\omega_p \Gamma_j}.$$

The nonlinear susceptibilities of the second $\chi^{(2)}$ and third $\chi^{(3)}$ orders have a much stronger dispersion in the polariton part of the spectrum. The dispersion $\chi^{(2)}$ is discussed in Sec. 5.a and the information on the dispersion of $\chi^{(3)}$ for the case under discussion can be found, for example, in Refs. 144, 145, and 147. The nonlinear susceptibility $\chi^{(3)}$ represents the contribution of direct four-photon processes to the intensity of the CARS signal, whereas $\chi^{(2)}$ represents the contribution of cascade or two-stage processes. A direct four-photon process is mixing of radiation fields from three lasers in such a way that $\omega_a = 2\omega_1 - \omega_2$ and the maximum intensity of this process is attained, according to Eqs. (8.1) and (8.2), when the phase-matching condition $\Delta k_a = 0$ is satisfied. It should be noted that polariton excitations do not appear in this process. Cascade processes are two sequential three-photon processes: a) creation of a polariton of frequency $\omega_p = \omega_1 - \omega_2$; b) creation of an anti-Stokes photon ω_a, accompanied by polariton annihilation: $\omega_a = \omega_1 + \omega_p = 2\omega_1 - \omega_2$. According to Eqs. (8.1) and (8.2) the highest efficiency of this process corresponds to the phase-matching conditions $\Delta k_p = 0$ and $\Delta k_a = 0$. In such a case the intensity of a CARS signal is governed by the polariton parameters since $\Delta \mathbf{k}_p = \mathbf{k}_1 - \mathbf{k}_2 - \mathbf{k}_p$. Since the maximum scattering intensity in the case of the cascade and direct processes is attained under different phase-matching conditions, it is possible to separate these two processes experimentally.[148]

It is interesting to note that because of the coherence of the scattering the various contributions of the direct and cascade processes are not summed but interfere, leading, generally speaking, to considerable distortion of the CARS spectra in the ω and k spaces. The influence of interference effects on CARS spectra is considered in Ref. 146 and demonstrated experimentally in Ref. 149 for an $LiIO_3$ crystal.

Figure 32 illustrates the influence of interference in the case of a CARS polariton spectrum obtained for an $LiIO_3$ crystal in k space for $\nu_1 - \nu_2 = 2300$ cm^{-1} (Ref. 149). This k spectrum was obtained by altering the directions of the wave vectors of the laser beams relative to the optical axis of a crystal: the investigated sample was rotated keeping the scattering geometry constant.

The considerable asymmetry and the presence of a "dip" in the spectrum in Fig. 32 are evidence of the interference effects in the CARS polariton spectra. The dashed curve in this figure is the calculated spectrum obtained theoretically.[146] This calculation is based on expressions corresponding to the case of weak pumping and weak polariton absorption attained in the experiments. It should be noted that the form of the spectrum depends strongly on the relative contributions of the direct and cascade processes governed by the ratio $\chi^{(3)}/[\chi^{(2)}]^2$. Clearly, interference disappears if we eliminate one of the scattering mechanisms. Therefore, the value of the ratio $\chi^{(3)}/[\chi^{(2)}]^2$ is selected in such a way as to obtain the best possible agreement between the experimental and calculated data.

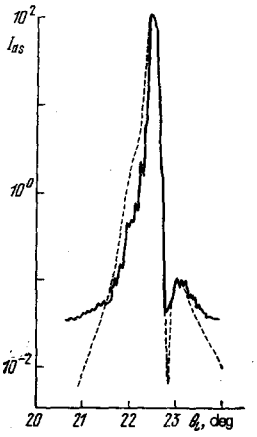

FIG. 32. Coherent anti-Stokes Raman scattering (CARS) spectrum in k space. The continuous curve is experimental and the dashed curve is calculated. Here, θ_L is the angle between the wave vector $\mathbf{k}_1$ and the optical axis of the crystal; I_{as} is the intensity of a CARS signal in relative units.

It follows that a correct interpretation of the CARS polariton spectra requires allowance for the possibility of the appearance of several maxima or of asymmetry of the line profile due to interference between direct and cascade processes. Moreover, the profile of a CARS line can be used to determine the absolute sign and relative magnitude of the ratio $\chi^{(3)}/[\chi^{(2)}]^2$.

An important application of CARS spectroscopy is the investigation of surface polaritons. The point is that a study of surface polaritons by the Raman scattering method involves a number of difficulties due to the fact that the scattering of light by bulk polaritons masks the weaker scattering by surface polaritons.[88] Therefore, it is not possible to observe the Raman scattering of light by surface polaritons in bulk samples. Only one experiment was carried out in which the Raman scattering of light by surface polaritons was observed and the sample was not of the bulk type.[150] In this experiment the intensity of the scattering of light by bulk polaritons was minimized by the use of thin (~2500 Å) single-crystal GaAs films grown epitaxially on a sapphire substrate. However, it is difficult to prepare thin single-crystal films. One also has to ensure that the phonon spectrum of the substrate is sufficiently far from the spectrum of surface polaritons of the investigated film.

Selective coherent excitation of surface polaritons occurs in CARS spectroscopy and, therefore, the intensity of the signal can be considerably higher than the intensity of the spontaneous Raman scattering by bulk polaritons[151,152] and this makes it possible to investigate surface polaritons in bulk samples. The first successful observation of surface polaritons in a bulk crystal of GaP was made by the CARS spectroscopy method.[152] Thus, CARS spectroscopy will undoubtedly become a very effective method for investigating surface states.[12)]

It is interesting to mention also the possibility of a

[12)]The method of compensation of the nonresonance background in CARS spectra proposed in Ref. 165 may be useful in such investigations.

direct measurement of the dephasing times of polariton excitations by the CARS spectroscopy method. For example, if the exciting fields ω_1 and ω_2 are suddenly removed, a CARS signal decays in a time T_2 needed for dephasing of polaritons originally phase-locked by the fields ω_1 and ω_2. Thus, in contrast to the conventional Raman scattering, CARS is due to the polarization of the medium at the frequency ω_p and not due to the level populations. The relaxation and excitation dephasing times can be measured using a laser generating ultrashort pulses.[155] Two lasers generating ultrashort pulses excite polaritons and a test beam is then sent to a crystal after some delay. The dependence of the intensity of a CARS signal on the delay of a test pulse is used to find the dephasing time T_2. Measurements of the corresponding dependence of the intensity of noncoherent Raman scattering of light can be used to determine also the longitudinal relaxation time T_1. The first successful measurement of the lifetime of a polariton mode in GaP was made near the frequency of a transverse optical phonon[156] and the lifetime was found to be 5.5 ± 0.5 psec.

9. CONCLUSIONS

Raman scattering of light by polaritons makes it possible to determine directly the dispersion of the permittivity over a wide spectral range (from a few to a few thousand reciprocal centimeters) and it is very useful in studies of the fundamental vibrations of the crystal lattice.[13)] Spectroscopy of the Raman scattering of light by optical phonons makes it possible to obtain information on the permittivity dispersion only if the harmonic oscillator model is used. However, investigations of the polariton scattering spectra under Fermi resonance conditions show, for example, that the anharmonicity effects may have a considerable influence on the dispersion of the permittivity, at least in the region of overtones and combination frequencies of the lattice vibrations. Experimental investigations of polariton Fermi resonances are still in the initial stage and are mainly descriptive. A fuller understanding of this interesting phenomenon requires that the investigations should reach a level at which quantitative comparisons can be made between the theoretical and experimental results.

Low-angle Raman spectroscopy makes it possible to investigate the spectra of elementary excitations and to reveal changes which appear as a result of interaction between various excitations. An increase in the intensity of scattering of light by excitations with a small scattering cross section in the region of intersection between polariton branches may play an important role in the detection of excitations which are weak in the Raman sense. There are no basic restrictions on the possibility of detection of polaritons accompanied by generation of "new" waves in optically active crystals[93] and magnon polaritons.[157] Polariton scattering spectra of ferroelectrics can yield valuable information on phase transitions in these crystals.[10,17,27,44,118,119,158,166] In particular, the low-angle Raman scattering method is promising for the study of relaxation processes near phase transitions.[159] Coherent anti-Stokes Raman scattering of light will become an effective method for investigating surface excitations.

From the practical point of view, the spontaneous low-angle Raman scattering is an effective instrument in the search for materials in which the stimulated Raman scattering by polaritons may be observed. The results of recent investigations[160] indicate that frequency-tunable far infrared sources based on the stimulated Raman scattering by polaritons may have parameters which would make them suitable for experimental investigations.

It is clear from the above discussions that low-angle Raman scattering spectroscopy is an extremely promising method[9,100,161,162,164] for tackling a number of problems in solid state physics.

[13)] The majority of the published experimental investigations deals with these problems.

[1] C. H. Henry and J. J. Hopfield, Phys. Rev. Lett. **15**, 964 (1965).
[2] S. P. S. Porto, B. Tell, and T. C. Damen, Phys. Rev. Lett. **16**, 450 (1966).
[3] S. Ushioda and J. D. McMullen, Solid State Commun. **11**, 299 (1972).
[4] C. K. N. Patel, and R. E. Slusher, Phys. Rev. Lett. **22**, 282 (1969).
[5] A. D'Andrea, B. Fornari, G. Mattei, M. Pagannone, and M. Scrocco, Phys. Status Solidi B **54**, K131 (1972).
[6] A. V. Bobrov and M. Krauzman, J. Raman Spectrosc. **1**, 365 (1973).
[7] G. G. Mitin, V. S. Gorelik, L. A. Kulevskiĭ, Yu. N. Polivanov, and M. M. Sushchinskiĭ, Zh. Eksp. Teor. Fiz. **68**, 1757 (1975) [Sov. Phys. JETP **41**, 882 (1975)].
[8] V. S. Gorelik, G. G. Mitin, and M. M. Sushchinskiĭ, Zh. Eksp. Teor. Fiz. **68**, 823 (1975) [Sov. Phys. JETP **42**, 419 (1975)].
[9] R. Claus, Phys. Status Solidi B **50**, 11 (1972).
[10] J. F. Scott, P. A. Fleury, and J. M. Worlock, Phys. Rev. **177**, 1288 (1968).
[11] J. F. Scott, L. E. Cheesman, and S. P. S. Porto, Phys. Rev. **162**, 834 (1967).
[12] J. Fries and R. Claus, J. Raman Spectrosc. **1**, 71 (1973).
[13] H. E. Puthoff, R. H. Pantell, B. G. Huth, and M. A. Chacon, J. Appl. Phys. **39**, 2144 (1968).
[14] D. N. Klyshko, A. N. Penin, and B. F. Polkovnikov, Pis'ma Zh. Eksp. Teor. Fiz. **11**, 11 (1970) [JETP Lett. **11**, 5 (1970)].
[15] R. Claus, G. Borstel, and L. Merten, Opt. Commun. **3**, 17 (1971).
[16] F. X. Winter and R. Claus, Opt. Commun. **6**, 22 (1972).
[17] M. Rokni, L. S. Wall, E. Amzallag, and T. S. Chang, Solid State Commun. **10**, 103 (1972).
[18] M. Posledovich, F. X. Winter, R. Claus, and G. Borstel, Phys. Status Solidi B **55**, 711 (1973).
[19] B. N. Mavrin, T. E. Abramovich, and Kh. E. Sterin, Fiz. Tverd. Tela (Leningrad) **14**, 1810, 3054 (1972) [Sov. Phys. Solid State **14**, 1562 (1972); **14**, 2611 (1973)].
[20] B. N. Mavrin and Kh. E. Sterin, Pis'ma Zh. Eksp. Teor. Fiz. **16**, 265 (1972) [JETP Lett. **16**, 187 (1972)].
[21] G. M. Georgiev, G. Kh. Kitaeva, A. G. Mikhaĭlovskiĭ, A. N. Penin, and N. M. Rubinina, Fiz. Tverd. Tela (Leningrad) **16**, 3524 (1974) [Sov. Phys. Solid State **16**, 2302 (1975)].
[22] O. A. Aktsipetrov, G. M. Georgiev, A. G. Mikhaĭlovskiĭ,

A. N. Penin, Fiz. Tverd. Tela (Leningrad) **18**, 665 (1976) [Sov. Phys. Solid State **18**, 384 (1976)].
[23]J. H. Nicola, J. A. Freitas Jr., and R. C. C. Leite, Solid State Commun. **17**, 1379 (1975).
[24]A. Pinczuk, E. Burstein, and S. Ushioda, Solid State Commun. **7**, 139 (1969).
[25]G. Burns, Phys. Lett. A **43**, 271 (1973).
[26]L. Laughman, L. W. Davis, and T. Nakamura, Phys. Rev. **B6**, 3322 (1972).
[27]D. Heiman and S. Ushioda, Phys. Rev. **B9**, 2122 (1974).
[28]R. Claus, H. W. Schrotter, and H. H. Hacker, Z. Naturforsch. Teil A **24**, 1733 (1969).
[29]R. Claus, Z. Naturforsch, Teil A **25**, 306 (1970).
[30]C. K. Asawa and M. K. Barnoski, Phys. Rev. **B3**, 2682 (1971).
[31]W. Otaguro, E. Wiener-Avnear, C. A. Arguello, and S. P. S. Porto, Phys. Rev. **B4**, 4542 (1971).
[32]W. S. Otaguro, E. Wiener-Avnear, S. P. S. Porto, and J. Smit, Phys. Rev. **B6**, 3100 (1972).
[33]F. X. Winter, Phys. Lett. A **40**, 425 (1972).
[34]G. F. Dobrzhanskiĭ (V. F. Kitaeva, N. I. Krindach, L. A. Kulevskiĭ,) Yu. N. Polivanov, and S. N. Poluéktov, Kvantovaya Elektron. (Moscow) No. 3, 95 (1973) [Sov. J. Quantum Electron. **3**, 236 (1973)]; G. F. Dobrzhanskiĭ (Dobrzhansky), V. F. Kitaeva, N. I. Krindach, L. A. Kulevskiĭ (Kulevsky), Yu. N. Polivanov, and S. N. Poluektov, in: Polaritons (Proc. First Taormina Research Conf. on Structure of Matter, 1972, ed. by E. Burstein and F. De Martini), Pergamon Press, New York (1974), p. 65.
[35]K. D. Kneipp, H. E. Ponath, V. L. Strizhevskiĭ, and Yu. N. Yahskir, Pis'ma Zh. Eksp. Teor. Fiz. **18**, 89 (1973) [JETP Lett. **18**, 50 (1973)].
[36]K. D. Kneipp, R. Kuhmstedt, and H. E. Ponath, Exp. Tech. Phys. **21**, 403 (1973).
[37]L. A. Kulevskiĭ (Kulevsky), Yu. N. Polivanov, and S. N. Poluektov, J. Raman Spectrosc. **3**, 239 (1975); Proc. Third Intern. Conf. on Light Scattering in Solids, Campinas, Brazil, 1975 (ed. by M. Balkanski, R. C. C. Leite, and S. P. S. Porto), publ. by Flammarion Sciences, Paris; Halsted, New York (1976), p. 462.
[38]H. E. Ponath and K. D. Kneipp, Opt. Spektrosk. **38**, 696 (1975) [Opt. Spectrosc. (USSR) **38**, 394 (1975)].
[39]L. A. Kulevskiĭ (Kulevsky), Yu. N. Polivanov, and S. N. Poluektov, J. Raman Spectrosc. **5**, 269 (1976).
[40]K. Kneipp, W. Werncke, H. E. Ponath, J. Klein, A. Lau, and Chu Dinh Thuy, Phys. Status Solidi B **64**, 589 (1974).
[41]R. C. C. Leite, T. C. Damen, and J. F. Scott, Proc. First Intern. Conf. on Light Scattering Spectra in Solids, New York, 1968 (ed. by G. B. Wright), Springer Verlag, New York (1969), p. 359.
[42]J. H. Nicola and R. C. C. Leite, Phys. Rev. **B11**, 798 (1975).
[43]Z. M. Khaskhozhev, V. V. Lemanov, and R. V. Pisarev, Fiz. Tverd. Tela (Leningrad) **12**, 1208 (1970) [Sov. Phys. Solid State **12**, 941 (1970)].
[44]T. S. Chang, B. C. Johnson, E. Amzallag, R. H. Pantell, M. Rokni, and L. S. Wall, Opt. Commun. **4**, 72 (1971).
[45]O. A. Aktsipetrov, G. M. Georgiev, I. V. Mityusheva, A. G. Mikhaĭlovskiĭ, and A. N. Penin, Fiz. Tverd. Tela (Leningrad) **17**, 1508 (1975) [Sov. Phys. Solid State **17**, 983 (1975)].
[46]R. Claus, Phys. Lett. A **31**, 299 (1970).
[47]R. Claus and H. W. Schrotter, Opt. Commun. **2**, 105 (1970).
[48]V. V. Obukhovskiĭ and V. L. Strizhevskiĭ, Ukr. Fiz. Zh. **14**, 1463 (1969); Zh. Eksp. Teor. Fiz. **57**, 520 (1969) [Sov. Phys. JETP **30**, 285 (1970)].
[49]R. Claus, W. Nitsh, and J. Brandmuller, Proc. Third Intern. Conf. on Light Scattering in Solids, Campinas, Brazil, 1975 (ed. by M. Balkanski, R. C. C. Leite, and S. P. S. Porto), publ. by Flammarion Sciences, Paris; Halsted, New York (1976), p. 571.
[50]J. Shah, T. C. Damen, J. F. Scott, and R. C. C. Leite, Phys. Rev. **3**, 4238 (1971).
[51]J. F. Scott, T. C. Damen, and J. Shah, Opt. Commun. **3**, 384 (1971).
[52]L. Laughman and L. W. Davis, Phys. Rev. **B10**, 2590 (1974).
[53]A. A. Abdullaev, A. V. Vasil'eva, G. F. Dobrzhanskiĭ, and Yu. N. Polivanov, Kvantovaya Elektron. (Moscow) **4**, 108 (1977) [Sov. J. Quantum Electron. **7**, 56 (1977)].
[54]F. V. Kitaeva, L. A. Kulevskiĭ, Yu. N. Polivanov, and S. N. Poluéktov, Pis'ma Zh. Eksp. Teor. Fiz. **16**, 23 (1972) [JETP Lett. **16**, 15 (1972)]; V. F. Kitaeva, L. A. Kulevskiĭ (Kulevsky), Yu. N. Polivanov, and S. N. Poluektov, in: Polaritons (Proc. First Taormina Research Conf. on Structure of Matter, 1972, ed. by E. Burstein and F. De Martini), Pergamon Press, New York (1974), p. 69.
[55]D. N. Klyshko, V. F. Kutsov, A. N. Penin, and B. F. Polkovnikov, Zh. Eksp. Teor. Fiz. **62**, 1846 (1972) [Sov. Phys. JETP **35**, 960 (1972)].
[56]V. F. Kitaeva, L. A. Kulevskiĭ, Yu. N. Polivanov, and S. N. Poluéktov, Dokl. Akad. Nauk SSSR **107**, 1322 (1972) [Sov. Phys. Dokl. **17**, 1189 (1973)].
[57]G. M. Georgiev, A. G. Mikhaĭlovskiĭ, A. N. Penin, and V. N. Chumash, Fiz. Tverd. Tela (Leningrad) **16**, 2907 (1974) [Sov. Phys. Solid State **16**, 1882 (1975)].
[58]B. N. Mavrin and Kh. E. Sterin, Fiz. Tverd. Tela (Leningrad) **14**, 2774 (1972) [Sov. Phys. Solid State **14**, 2402 (1973)].
[59]G. Burns, Appl. Phys. Lett. **20**, 230 (1972).
[60]M. Yamamoto, H. Ito, and H. Inaba, Phys. Lett. A **55**, 303 (1975).
[61]G. S. Belikova, L. A. Kulevskiĭ (Kulevsky), Yu. N. Polivanov, S. N. Poluektov, K. A. Prokhorov, V. D. Shigorin, and G. P. Shipulo, J. Raman Spectrosc. **2**, 493 (1974).
[62]V. F. Zolin and M. A. Samokhina, Fiz. Tverd. Tela (Leningrad) **17**, 2774 (1975) [Sov. Phys. Solid State **17**, 1845 (1975)].
[63]F. X. Winter, E. Wiesendanger, and R. Claus, Phys. Status Solidi B **64**, 95 (1974).
[64]T. Fukumoto, A. Okamoto, T. Hattori, A. Mitsuishi, and T. Fukuda, Solid State Commun. **17**, 427 (1975).
[65]F. X. Winter, E. Wiesendanger, and R. Claus, Phys. Status Solidi B **72**, 189 (1975).
[66]D. G. Bozinis and A. Scalabrin, Proc. Third Intern. Conf. on Light Scattering in Solids, Campinas, Brazil, 1975 (ed. by M. Balkanski, R. C. C. Leite, and S. P. S. Porto), publ. by Flammarion Sciences, Paris; Halsted, New York (1976), p. 856.
[67]R. Claus and F. X. Winter, Proc. Third Intern. Conf. on Light Scattering in Solids, Campinas, Brazil, 1975 (ed. by M. Balkanski, R. C. C. Leite, and S. P. S. Porto), publ. by Flammarion Sciences, Paris; Halsted, New York (1976), p. 485.
[68]S. Ushioda, D. Heiman, and J. P. Remeika, Proc. Third Intern. Conf. on Light Scattering in Solids, Campinas, Brazil, 1975 (ed. by M. Balkanski, R. C. C. Leite, and S. P. S. Porto), publ. by Flammarion Sciences, Paris; Halsted, New York (1976), p. 457.
[69]M. Born and K. Huang, Dynamical Theory of Crystal Lattices, Oxford University Press, 1954 (Russ. Transl., IL, M., 1958).
[70]H. Poulet and J. P. Mathieu, Vibrational Spectra and Symmetry of Crystals, Gordon and Breach, Paris, 1970 (Russ. Transl., Mir, M., 1973).
[71]A. S. Barker Jr, Phys. Rev. **136**, A1290 (1964).
[72]R. Loudon, Adv. Phys. **13**, 423 (1964).
[73]L. Merten, Z. Naturforsch. Teil A **16**, 447 (1961).
[74]G. Lamprecht and L. Merten, Phys. Status Solidi **35**, 353 (1969).

[75]L. Merten, Phys. Status Solidi **30**, 449 (1968).
[76]S. J. Fray, F. A. Johnson, R. Jones, S. Kay, E. R. Pike, J. Russell, C. Sennett, and J. O'Shaughnessey, Proc. First Intern. Conf. on Light Scattering Spectras in Solids, New York 1968 (ed. by G. B. Wright), Springer Verlag, New York (1969), p. 139.
[77]W. L. Bond, J. Appl. Phys. **36**, 1674 (1965).
[78]G. F. Dobrzhanskiĭ, L. A. Kulevskiĭ, Yu. N. Polivanov, and K. A. Prokhorov, Kratk. Soobshch. Fiz. No. 11, 27 (1977).
[79]S. Umegaki, S. I. Tanaka, T. Uchiyama, and S. Yabumoto, Opt. Commun. **3**, 244 (1971).
[80]L. I. Kuznetsova, L. A. Kulevskiĭ, Yu. N. Polivanov, and K. A. Prokhorov, Kvantovaya Elektron. (Moscow) **2**, 2095 (1975) [Sov. J. Quantum Electron. **5**, 1146 (1975)]; L. I. Kuznetsova, L. A. Kulevskiĭ (Kulevsky), Yu. N. Polivanov, and K. A. Prokhorov, Proc. Third Intern. Conf. on Light Scattering in Solids, Campinas, Brazil, 1975 (ed. by M. Balkanski, R. C. C. Leite, and S. P. S. Porto), publ. by Flammarion Sciences, Paris; Halsted, New York (1976), p. 494.
[81]O. A. Aktsipetrov, G. M. Georgiev, I. V. Mityusheva, A. G. Mikhaĭlovskiĭ, and A. N. Penin, Fiz. Tverd. Tela (Leningrad) **17**, 2027 (1975) [Sov. Phys. Solid State **17**, 1324 (1975)].
[82]M. Born and E. Wolf, Principles of Optics, 3rd ed., Pergamon Press, Oxford, 1965 (Russ. Transls., Nauka, M., 1970).
[83]S. E. Harris, Proc. IEEE **57**, 2096 (1969).
[84]J. F. Scott, Rev. Mod. Phys. **46**, 83 (1974).
[85]E. R. Mustel' and V. N. Parygin, Metody modulyatsii i skanirovaniya sveta (Light Modulation and Scanning Methods), Nauka, M., 1970.
[86]M. V. Belousov, Fiz. Tverd. Tela (Leningrad) **15**, 1206 (1973) [Sov. Phys. Solid State **15**, 813 (1973)].
[87]V. V. Bryksin, D. N. Mirlin, and Yu. A. Firsov, Usp. Fiz. Nauk **113**, 29 (1974) [Sov. Phys. Usp. **17**, 305 (1974)].
[88]V. M. Agranovich, Usp. Fiz. Nauk **115**, 199 (1975) [Sov. Phys. Usp. **18**, 99 (1975)].
[89]A. S. Sonin and A. S. Vasil'eva, Élektrooptícheskie kristally (Electrooptic Crystals), Atomizdat, M., 1971.
[90]G. V. Krivoshchekov, S. V. Kruglov, S. I. Marennikov, and Yu. N. Polivanov, Pis'ma Zh. Eksp. Teor. Fiz. **7**, 84 (1968) [JETP Lett. **7**, 63 (1968)].
[91]G. V. Krivoshchekov, S. V. Kruglov, S. I. Marennikov, and Yu. N. Polivanov, Zh. Eksp. Teor. Fiz. **55**, 802 (1968) [Sov. Phys. JETP **28**, 415 (1969)].
[92]H. J. Benson and D. L. Mills, Phys. Rev. **B1**, 4835 (1970).
[93]V. M. Agranovich and V. L. Ginzburg, Zh. Eksp. Teor. Fiz. **61**, 1243 (1971) [Sov. Phys. JETP **34**, 662 (1972)].
[94]C. H. Henry and C. G. B. Garrett, Phys. Rev. **171**, 1058 (1968).
[95]J. P. Budin, B. Godard, and J. Ducuing, IEEE J. Quantum Electron. **QE-4**, 831 (1968).
[96]V. L. Strizhevskiĭ and V. V. Obukhovskiĭ, Zh. Eksp. Teor. Fiz. **58**. 929 (1970) [Sov. Phys. JETP **31**, 500 (1970)].
[97]V. V. Obukhovskiĭ, H. Ponath, and V. L. Strizhevskiĭ, Phys. Status Solidi **41**, 837 (1970).
[98]V. L. Strizhevskiĭ, Yu. N. Yashkir, and H. E. Ponath, Phys. Status Solidi B **69**, 673 (1975).
[99]V. V. Obukhovskiĭ, H. Ponath, and V. L. Strizhevskiĭ, Phys. Status Solidi B **41**, 847 (1970).
[100]A. S. Barker and R. Loudon, Rev. Mod. Phys. **44**, 18 (1972).
[101]R. Loudon, Proc. First Intern. Conf. on Light Scattering Spectra in Solids, New York, 1968 (ed. by G. B. Wright), Springer Verlag, New York (1969), p. 25.
[102]E. Burstein, S. Ushioda, and A. Pinczuk, Solid State Commun. **6**, 407 (1968).
[103]E. Burstein, S. Ushioda, A. Pinczuk, and J. F. Scott, Proc. First Intern. Conf. on Light Scattering Spectra in Solids, New York, 1968 (ed. by G. B. Wright), Springer Verlag, New York (1969), p. 43.
[104]S. Ushioda, A. Pinczuk, E. Burstein, and D. L. Mills, Proc. First Intern. Conf. on Light Scattering Spectra in Solids, New York, 1968 (ed. by G. B. Wright), Springer Verlag, New York (1969), p. 347.
[105]G. V. Krivoshchekov, S. I. Marennikov, and V. A. Orlov, Tezisy dokladov VII Vsesoyuznoĭ konferentsii po kogerentnoĭ i nelineĭnoĭ optike (Abstracts of Papers presented at Seventh All-Union Conf. on Coherent and Nonlinear Optics), Tashkent, 1974, p. 261.
[106]R. Claus, Rev. Sci. Instrum. **42**, 341 (1971).
[107]V. L. Strizhevskiĭ, Vis. Akad. Nauk Ukr. RSR No. 5, 22 (1971); V. L. Strizhevskiĭ, H. Ponath, and V. V. Obukhovskiĭ, Proc. Intern. Conf. on Lasers and Their Applications, Dresden, 1970, p. 1081.
[108]S. A. Akhmanov and R. V. Khokhlov, Problemy nelineĭnoĭ Optiki (Problems in Nonlinear Optics), Izd. AN SSSR, M., 1964.
[109]V. M. Faĭn, Kvantovaya radiofizika, t. 1, Fotony i nelineĭnye sredy (Quantum Electronics, Vol. 1, Photons and Nonlinear Media), Sovet-skoe Radio, M., 1973.
[110]N. Bloembergen, Nonlinear Optics, Benjamin, New York, 1965 (Russ. Transl., Mir, M., 1965).
[111]A. Yariv, Quantum Electonics, Wiley, New York, 1967 (Russ. Transl., Sovet-skoe Rakio, M., 1973).
[112]F. Zernike and J. E. Midwinter, Applied Nonlinear Optics: Basics and Applications, Interscience, New York, 1973 (Russ. Transl., Mir, M., 1976).
[113]A. F. Penna, A. Chaves, P. da R. Andrade, and S. P. S. Porto, Phys. Rev. **B13**, 4907 (1976).
[114]S. A. Akhmanov, V. A. Fadeev, R. V. Khokhlov, and O. N. Chunaev, Pis'ma Zh. Eksp. Teor. Fiz. **6**, 575 (1967) [JETP Lett. **6**, 85 (1967)].
[115]D. N. Klyshko and D. P. Krindach, Zh. Eksp. Teor. Fiz. **54**, 697 (1968) [Sov. Phys. JETP **27**, 371 (1968)].
[116]S. E. Harris, M. K. Oshman, and R. L. Byer, Phys. Rev. Lett. **18**, 732 (1967).
[117]D. Magde and H. Mahr, Phys. Rev. Lett. **18**, 905 (1967).
[118]Y. Tominaga and T. Nakamura, Solid State Commun. **15**, 1193 (1974).
[119]Y. Tominaga and T. Nakamura, J. Phys. Soc. Jpn. **39**, 746 (1975).
[120]A. Ben-Amar and E. Wiener-Avnear, Appl. Phys. Lett. **27**, 410 (1975).
[121]W. D. Johnston Jr. and I. P. Kaminow, Phys. Rev. **188**, 1209 (1969).
[122]A. Mooradian and A. L. McWhorter, Proc. First Intern. Conf. on Light Scattering Spectra in Solids, New York, 1968 (ed. by G. B. Wright), Springer Verlag, New York (1969), p. 297.
[123]W. L. Faust and C. H. Henry, Phys. Rev. Lett. **17**, 1265 (1966).
[124]W. L. Faust, C. H. Henry, and R. H. Eick, Phys. Rev. **173**, 781 (1968); O. Brafman and S. S. Mitra, Phys. Rev. **171**, 931 (1968).
[125]T. C. Damen, S. P. S. Porto, and B. Tell, Phys. Rev. **142**, 570 (1966).
[126]G. P. Montgomery Jr and T. C. Giallorenzi, Phys. Rev. **B8**, 808 (1973).
[127]B. B. Varga, Phys. Rev. **137**, A1896 (1965).
[128]L. É. Gurevich and R. G. Tarkhanyan, Fiz. Tekh. Poluprovodn. **6**, 1895 (1972) [Sov. Phys. Semicond. **6**, 1631 (1973)].
[129]P. A. Wolff, Phys. Rev. **B1**, 950 (1970); F. A. Blum, Phys. Rev. **B1**, 1125 (1970).
[130]K. Ohtaka, Phys. Status Solidi B **57**, 51 (1973).
[131]W. Nitsch and R. Claus, Z. Naturforsch. Teil A **29**, 1017 (1974).
[132]R. Claus, G. Borstel, E. Wiesendanger, and L. Steffan, Z. Naturforsch. Teil A **27**, 1187 (1972).
[133]K. B. Harvey and N. R. McQuaker, J. Chem. Phys. **55**,

4390 (1971).
[134]G. G. Mitin, V. S. Gorelik, and M. M. Sushchinskiĭ, Fiz. Tverd. Tela (Leningrad) **16**, 2956 (1974) [Sov. Phys. Solid State **16**, 1912 (1975)].
[135]V. M. Agranovich and I. I. Lalov, Solid State Commun. **19**, 503 (1976).
[136]W. Nitsch, Z. Naturforsch. Teil A **30**, 537 (1975).
[137]D. L. Mills and A. A. Maradudin, Phys. Rev. **B1**, 903 (1970).
[138]A. A. Maradudin and J. Oitmaa, Solid State Commun. **7**, 1143 (1969); A. D'Andrea, B. Fornari, G. Mattei, L. Mattioli, and M. Pagannone, Solid State Commun. **18**, 949 (1976).
[139]R. Fischer and L. A. Kulevskiĭ, Kvantovaya Elektron. (Moscow) **4**, 245 (1977) [Sov. J. Quantum Electron. **7**, 135 (1977)].
[140]V. M. Agranovich, Suppl. to H. Poulet and J. P. Mathieu, Vibrational Spectra and Symmetry of Crystals, Gordon and Breach, Paris, 1970 (Russ. Transl., Mir, M., 1973), p. 408.
[141]M. H. Cohen and J. Ruvalds, Phys. Rev. Lett. **23**, 1378 (1969); J. Ruvalds and A. Zawadowski, Phys. Rev. **B2**, 1172 (1970); K. L. Ngai, A. K. Ganguly, and J. Ruvalds, Phys. Rev. **B10**, 3280 (1974).
[142]A. S. Pine and A. G. Dresselhaus, Phys. Rev. **B188**, 1489 (1969).
[143]J. P. Coffinet and F. De Martini, Phys. Rev. Lett. **22**, 60 (1969); F. De Martini and J. Leroy, Solid State Commun. **9**, 1779 (1971).
[144]J. J. Wynne, Phys. Rev. Lett. **29**, 650 (1972).
[145]J. J. Wynne, Comments Solid State Phys. **7**, 7 (1972).
[146]V. L. Strizhevskiĭ and Yu. N. Yashkir, Kvantovaya Elektron. (Moscow) **2**, 995 (1975) [Sov. J. Quantum Electron. **5**, 541 (1975)].
[147]D. N. Klyshko, Kvantovaya Elektron. (Moscow) **2**, 265 (1975) [Sov. J. Quantum Electron. **5**, 149 (1975)].
[148]Yu. N. Polivanov, R. Sh. Sayakhov, and A. T. Sukhodol'skiĭ, Kratk. Soobshch. Fiz. No. 12, 16 (1976).
[149]Yu. N. Polivanov and A. T. Sukhodol'skiĭ, Pis'ma Zh. Eksp. Teor. Fiz. **25**, 240 (1977) [JETP Lett. **25**, 221 (1977)].
[150]D. J. Evans, S. Ushioda, and J. D. McMullen, Phys. Rev. Lett. **31**, 369 (1973); J. Y. Prieur and S. Ushioda, Phys. Rev. Lett. **34**, 1012 (1975).
[151]N. I. Likholit, V. L. Strizhevskiĭ and Yu. N. Yashkir, Kvantovaya Elektron. (Moscow) **3**, 457 (1976) [Sov. J. Quantum Electron. **6**, 250 (1976)]; N. N. Akhmediev, Kvantovaya Elektron. (Moscow) **3**, 1354 (1976) [Sov. J. Quantum Electron. **6**, 738 (1976)]; F. De Martini and Y. R. Shen, Phys. Rev. Lett. **36**, 216 (1976).
[152]F. De Martini, G. Giuliani, P. Mataloni, E. Palange, and Y. R. Shen, Phys. Rev. Lett. **37**, 440 (1976).
[153]S. A. Akhmanov and N. I. Koroteev, Zh. Eksp. Teor. Fiz. **67**, 1306 (1974) [Sov. Phys. JETP **40**, 650 (1975)].
[154]T. A. Leskova, B. N. Mavrin, and Kh. E. Sterin, Fiz. Tverd. Tela (Leningrad) **18**, 3653 (1976) [Sov. Phys. Solid State **18**, 2127 (1976)].
[155]A. Laubereau and W. Kaiser, Opto-electronics **6**, 1 (1974).
[156]A. Laubereau, D. Von der Linde, and W. Kaiser, Opt. Commun. **7**, 173 (1973).
[157]C. Manohar and G. Venkataraman, Phys. Rev. **B5**, 1993 (1972); E. F. Sarmento and D. R. Tilley, J. Phys. C **9**, 2943 (1976).
[158]O. A. Aktsipetrov, G. Kh. Kitaeva, and A. N. Penin, Fiz. Tverd. Tela (Leningrad) **19**. 1001 (1977) [Sov. Phys. Solid State **19**, 582 (1977)].
[159]L. Merten and P. da R. Andrade, Phys. Status Solidi B **62**, 641 (1974).
[160]M. A. Piestrup, R. N. Fleming, and R. H. Pantell, Appl. Phys. Lett. **26**, 418 (1975).
[161]J. F. Scott, Am. J. Phys. **39**, 1360 (1971).
[162]R. Claus, L. Merten, and J. Brandmuller, Light Scattering by Phonon Polaritons (Springer Tracts in Modern Physics, No. 75), Springer Verlag, Berlin, 1975.
[163]V. A. Vinokurov, S. S. Klyago, Yu. N. Polivanov, and K. A. Prokhorov, Kvantovaya Elektron. (Moscow) **4**, 1602 (1977) [Sov. J. Quantum Electron. **7**, 913 (1977)].
[164]R. Claus, Spectrosc. Lett. **9**, 575 (1976).
[165]Yu. N. Polivanov and A. T. Sukhodol'skiĭ, Pis'ma Zh. Tekh. Fiz. **4**, 164 (1978) [Sov. Tech. Phys. Lett. **4**, 67 (1978)].
[166]A. F. Penna, A. Chaves, and S. P. S. Porto, Solid State Commun. **19**, 491 (1976).

Translated by A. Tybulewicz